



Research Paper

BMP4-mediated browning of perivascular adipose tissue governs an anti-inflammatory program and prevents atherosclerosis

Wenjuan Mu^{a,1}, Shuwen Qian^{a,1}, Yanjue Song^a, Lijie Yang^a, Saisai Song^a, Qiqi Yang^a, Hao Liu^b, Yang Liu^a, Dongning Pan^a, Yan Tang^{a,**}, Qi-Qun Tang^{a,*}

^a Key Laboratory of Metabolism and Molecular Medicine, Ministry of Education, Department of Biochemistry and Molecular Biology of School of Basic Medical Sciences and Department of Endocrinology and Metabolism of Zhongshan Hospital, Fudan University, Shanghai 200032, China

^b Department of Cardiothoracic Surgery, Xinhua Hospital, Shanghai Jiaotong University of Medicine College, Shanghai 200032, China



ARTICLE INFO

Keywords:

Perivascular adipose tissue
Browning
Lipid metabolism
Inflammation
Atherosclerosis

ABSTRACT

Loss of perivascular adipose tissue (PVAT) impairs endothelial function and enhances atherosclerosis. However, the roles of PVAT thermoregulation in vascular inflammation and the development of atherosclerosis remains unclear. Bone morphogenetic protein 4 (BMP4) transforms white adipocyte to beige adipocyte, while promotes a brown-to-white shift in inter-scapular brown adipose tissue (BAT). Here, we found that knockdown of BMP4 in PVAT reduced expression of brown adipocyte-characteristic genes and increased endothelial inflammation in vitro co-culture system. Ablating BMP4 expression either in adipose tissues or specifically in BAT in ApoE^{-/-} mice demonstrated a marked exacerbation of atherosclerotic plaque formation in vivo. We further demonstrated that proinflammatory factors (especially IL-1 β) increased in the supernatant of BMP4 knockdown adipocytes. Overexpression of BMP4 in adipose tissues promotes browning of PVAT and protects against atherosclerosis in ApoE^{-/-} mice. These findings uncover an organ crosstalk between PVAT and blood endothelial cells that is engaged in atherosclerosis.

1. Introduction

Atherosclerosis is a chronic inflammatory disease intimately associated with metabolic syndrome [1,2]. The atherogenic process starts with the accumulation of lipoproteins in the subendothelial space and subsequent endothelial dysfunction [3,4]. Although multiple lines of incontrovertible evidence have proven a causal role for low-density lipoprotein (LDL) cholesterol in atherosclerosis, cardiovascular diseases still occur when LDL clearance is enhanced [5]. Increasing proof points to the role of inflammation as the culprit in atherosclerosis [6,7]. In metabolic syndrome, adipocytes secrete factors, such as free fatty acids and proinflammatory cytokines, which increase the risk of atherosclerosis [8]. Furthermore, a recent study demonstrated that murine perivascular adipose tissue (PVAT) is resistant to diet-induced macrophage infiltration, and thus may play an important role in protecting the vascular bed from inflammatory stress [9]. Although the concept that

inflammation plays a key role in the pathophysiology of atherosclerosis has gained considerable attention, its inciting has not yet been fully elucidated.

PVAT, as a local adipose tissue depot surrounding blood vessels, has emerged as an active component of the blood vessel wall and shares common features with brown adipose tissue (BAT) [10]. Several studies have demonstrated that activation of BAT metabolism significantly reduces the development of atherosclerosis due to low levels of plasma triglycerides and cholesterol [11–13]. Mild cold stimulation activates PVAT metabolism, that is, enhances thermoregulation of PVAT, which also has effect of resisting atherosclerosis [10]. Furthermore, overexpression of a mitochondrial membrane protein, mitoNEET, in PVAT has been shown to increase PVAT-dependent thermogenesis, leading to significantly downregulated PVAT inflammatory gene expression and reduced atherosclerosis [14]. Moreover, our previous study showed that uncoupling protein 1 (UCP1) and other brown-related proteins had

* Corresponding author. Department of Biochemistry and Molecular Biology, Fudan University Shanghai Medical College, Yi xue yuan Road, Shanghai 200032, PR China.

** Corresponding author. Department of Biochemistry and Molecular Biology, Fudan University Shanghai Medical College, Yi xue yuan Road, Shanghai 200032, PR China.

E-mail addresses: yantang@fudan.edu.cn (Y. Tang), qqtang@shmu.edu.cn (Q.-Q. Tang).

¹ These authors contributed equally to this work.

reduced expression in pericardial adipose tissue from patients with coronary artery disease (CAD) compared with non-CAD patients [15]. Consistently, Suho Kim et al. found that PVAT at atherosclerotic plaque sites typically showed agglomerated lipid droplets but decreased UCP1 in the advanced stage of atherosclerosis [16]. Therefore, impaired PVAT metabolism may be involved in CAD, and the underlying mechanisms require further investigation.

Bone morphogenetic protein 4 (BMP4) is an important regulator of adipogenesis by committing mesenchymal precursor cells into the adipogenic lineage [17]. BMP4 can induce UCP1 expression in human adipose stromal cells when combined with BMP7 and activate a full program of brown adipogenesis in C3H10T1/2 pluripotent cells [18,19]. Furthermore, we found that BMP4 also enhances browning of white adipocytes, as previously shown in transgenic mice overexpressing BMP4 in fat [20]. Mechanistically, overexpression of BMP4 in white adipose tissue (WAT) activates the p38/MAPK/ATF2/PGC1 α pathway. However, larger areas of BAT, with increased lipid droplet size and reduced UCP1 expression, were also found in BMP4 transgenic and AAV-BMP4-infusion animal models [21,22]. Thus, although BMP4 is known to exert different effects on WAT and BAT, the function of BMP4 on PVAT remains unclear.

Here, we report that the expression of BMP4 is high in normal PVAT, but decreased in murine and human PVAT with atherosclerosis. Moreover, adipocyte-specific loss of BMP4 promoted a brown-to-white transition in PVAT, and aggravated the inflammatory responses of endothelial cells, thereby promoting the development of atherosclerosis in apolipoprotein E deficient (ApoE^{-/-}) mice. By contrast, overexpression of BMP4 in adipocytes stimulated browning of PVAT, inhibited inflammatory responses, and protected against atherosclerosis. Furthermore, our results show that knockdown of BMP4 in adipocytes resulted in increased proinflammatory cytokine production, including tumor necrosis factor alpha (TNF α), interleukin 1 β (IL-1 β), interleukin 6 (IL-6) and C-C motif chemokine ligand 2 (CCL2/MCP1), all of which trigger endothelial cell inflammation. Collectively, our data suggest that BMP4 is a critical mediator of PVAT metabolism and protect against the development of atherosclerosis by inhibiting inflammation.

2. Materials and methods

2.1. Experimental design

The objective of this study was to investigate thermoregulation of PVAT in endothelial inflammation and the development of atherosclerosis. We treated HUVECs with conditioned medium from different brown adipocytes and measured the endothelial cell inflammation by Western blot and qPCR. We ablated BMP4 expression either in adipose tissues or specifically in BAT in ApoE^{-/-} mice to generate two types of BMP4-KO mice. We fed mice with a Western diet (WD) to induce atherosclerosis, examined the PVAT metabolic activity by performing IHC, Western blot and qPCR, and measured the development of atherosclerosis by performing Oil Red staining on the whole aorta and aortic sinus. To investigate whether overexpression of BMP4 in PVAT protect against atherosclerosis, we measured PVAT metabolic activity and atherosclerosis of BMP4-Tg ApoE^{-/-} mice. All mouse experiments were independently replicated at least twice. The cell culture experiments were performed using triplicates and repeated at least three times. We did not exclude any data points or mice unless a technical issue or a human error had occurred.

2.2. Human adipose tissue samples

Human adipose tissues were obtained from patients who underwent heart surgery in Shanghai Jiaotong University Affiliated Xinhua Hospital. Detailed information of regarding the patients is shown in [Supplemental Table S1](#). Briefly, samples were obtained from the following sites: epicardial adipose tissue (EAT) over the aortic root; paracardial

adipose tissue (PAT) from the inner midcourse and the diaphragm; and thoracic subcutaneous adipose tissue (SAT) from the sternotomy incision at the manubrium sterni. Fat samples were trimmed of connective tissue and superficial blood vessels, bisected, and stored separately at -80 °C until further processing. This study was approved by the Ethics Committees of Shanghai Medical College, Fudan University and was performed in accordance with the principle of the Helsinki Declaration II. Written informed consent was obtained from each participant.

2.3. Animals

To generate mice with an adipocyte-specific knockout of BMP4, BMP4^{fl/fl} mice (generously provided by Brigid Hogan, Department of Cell Biology, Duke University Medical Center, Durham, NC) were crossed with mice expressing Cre recombinase under the control of the adipocyte-specific promoter aP2/Fabp4 or UCP1. The generation of BMP4-Tg mice has been previously described [20]. Briefly, male ApoE^{-/-} mice were purchased from GemPharmatech Co., Ltd. For the atherosclerosis study, BMP4^{fl/fl}, BMP4 ^{Δ aP2} and BMP4 ^{Δ UCP1} were crossed with ApoE^{-/-} mice on the C57BL/6 background to produce BMP4^{fl/fl} ApoE^{-/-}, BMP4 ^{Δ aP2} ApoE^{-/-} and BMP4 ^{Δ UCP1} ApoE^{-/-} mice, respectively. Similarly, BMP4-Tg mice and their littermates were crossed with ApoE^{-/-} mice on the C57BL/6 background to produce BMP4-Tg ApoE^{-/-} and their control mice referred as ApoE^{-/-}. All mice were housed in a temperature-controlled animal facility (23 °C) with a 12 h:12 h light-dark cycle. All mice were given free access to water and rodent chow before a WD (42% fat, 0.2% total cholesterol, TD.88137; Harlan Teklad). Eight-week-old male BMP4^{fl/fl} ApoE^{-/-}, BMP4 ^{Δ aP2} ApoE^{-/-} and BMP4 ^{Δ UCP1} ApoE^{-/-} mice were fed a WD for 16 weeks to investigate the development of atherosclerosis. To investigate whether BMP4 in PVAT mediates a resistance to atherosclerosis, ApoE^{-/-} and BMP4 Tg ApoE^{-/-} mice were fed a WD for 20 weeks. The littermates were compared in all experiments described here. The old ApoE^{-/-} mice were 18 months old, and young ApoE^{-/-} mice were 2 months old. The old and young ApoE^{-/-} mice were fed with a chow diet. All of the studies were approved by the Animal Care and Use Committee of the Fudan University Shanghai Medical College, and followed the NIH guidelines on the care and use of animals.

2.4. Mouse PVAT sample collection

Samples (20 mg–40mg) were isolated from thoracic aortic PVAT, and stored at -80 °C until further processing.

2.5. Cell culture

Immortalized brown preadipocytes has been described previously [23].

Human umbilical vein endothelial cells (ScienCell Research Laboratories, San Diego, USA) were cultured on collagenase-coated dishes with endothelium cell basal medium (ScienCell Research Laboratories, San Diego, USA) containing 5% fetal bovine serum (FBS), streptomycin (100 IU/mL), penicillin (100 IU/mL) and amphotericin B (10 μ g/L). To activate endothelial cells and induce endothelial inflammation, HUVECs were treated with TNF α (10 ng/mL; Sino Biological, China) for 24 h before co-cultured experiments.

Human dermal fibroblasts (ScienCell Research Laboratories, San Diego, USA) were cultured using the human fibroblast growth medium (ScienCell Research Laboratories, San Diego, USA) containing 2% FBS, streptomycin (100 IU/mL) and penicillin (100 IU/mL).

Mouse C2C12 cell lines were purchased from American Type Culture Collection (ATCC, Manassas, VA, USA). C2C12 cells were cultured in growth medium (GM), which supplemented DMEM (Gibco, USA) with 10% fetal bovine serum and 1% penicillin-streptomycin (Biological Industries, Israel). To induce cell differentiation, culture medium was switched to differentiation medium (DM) with 2% horse serum and 1%

penicillin–streptomycin (Biological Industries, Israel). All cell lines were maintained at 37 °C with 5% CO₂ with corresponding medium.

2.6. Ex vivo fat tissue explant culture and co-culture experiments

The mice were sacrificed, and equal amounts of adipose tissues (inguinal, gonadal, BAT, and perivascular adipose tissue) were rinsed in phosphate-buffered saline (PBS) and incubated in Dulbecco's modified Eagle's medium or Ham's F12 medium (Gibco, USA). Co-culture experiments were conducted in 12-well transwell plates with 0.4- μ m pore-sized filters (Corning Costar, USA). Adipose tissues were placed in each transwell insert with HUVECs seeded onto the bottom chamber. Both adipose tissues and HUVECs were washed with PBS before the co-culture experiments.

2.7. Adenoviral expression vectors

The adenoviral expression vector pAd/CMV/V5-DEST (Invitrogen, Carlsbad, CA, USA) encoding *BMP4* was constructed according to the manufacturer's protocol. The *BMP4* sequence was amplified using the following primers 5'- ATGATTC CTGGTAACCGAA -3' (forward) and 5'- TCAGCGGCATCCACAC-3' (reverse). The adenoviral expression vector pBlock-it (Invitrogen, Carlsbad, CA, USA) encoding shRNA of the *BMP4* and *PGC1 α* genes was constructed according to the manufacturer's protocols. The sequence for sh*BMP4* was as following: CACCGGATTA-CATGAGGGATCTTTACGAATAAAGATCCCTCATGTAATCC. The sequence for sh*PGC1 α* has been previously described [20].

The brown adipocyte differentiation method is described in the cell culture section. On day 6, we infected the adipocytes (in 3.5 cm dishes) with 5000 PFU of adenovirus (Ad-shLacZ or Ad-sh*BMP4*, Ad-LacZ or Ad-*BMP4*, Ad-shLacZ or Ad-sh*PGC1 α*) supplemented with 8 μ g/mL of polybrene (Sigma, USA) to enhance adenovirus infection efficiency. The media was refreshed after 24 h, and after 48 h, the media was harvested as conditioned medium for further experiments.

2.8. RNA sequencing

Total RNA was purified from PVAT of *BMP4^{fl/fl} ApoE^{-/-}* and *BMP4 ^{Δ ap2} ApoE^{-/-}* mice. Each group had three mice. Uniquely indexed libraries were generated for each sample using the NEBNext Ultra™ RNA Library Prep Kit for Illumina (NEB, USA), according to the manufacturer's instructions. The indexed libraries were sequenced using the Illumina HiSeq platform, generating 125 bp long paired-end reads, yielding a minimum of ~20 million total reads per sample. After assessing sequence quality, STAR was used to map reads to the mouse genome (mm10) with default setting values. Mapping efficiency was >95% in all experiments. Then mapped reads were annotated, and the FPKM (fragments per kilo base per million mapped reads) was calculated with geneCode M19 annotation reference. A total of 10,818 protein-coding genes with FPKM \geq 1 were used for differential expression analysis with a fold change of 1.5 as a cutoff. The results demonstrated that 1218 genes were up-regulated and 410 genes were down-regulated in the *BMP4*-KO group. The altered genes were used for gene ontology analysis in KEGG pathways. Pathways with *p* value < 0.00015 were exported and visualized in Cytoscape v.3.4.0.

2.9. Collection of cell culture supernatants for proteomics

Immortalized brown preadipocytes were seeded in 3.5 cm dishes and induced to mature brown adipocytes. After a 6-day induction period, cells were treated with pAd-*BMP4* shRNA. 24 h later, the cells were washed three times with PBS, and then cultured in serum-free MEM medium (without phenol red [Gibco, USA]) supplemented with non-essential amino acids (NEAA) and L-glutamine. After 24 h serum-free culture, the supernatant was collected and filtered by MILLEX®-HP filter unit (0.45 μ m pore size, Merck Millipore Ltd.). The filtered

supernatant was concentrated by Amicon® Ultra-15 3K devices (Merck Millipore Ltd.). The concentrated supernatant samples were ready for proteomic analysis.

2.10. Quantitative PCR

Total RNA was extracted by TRIzol (Life Technologies, Carlsbad, CA, USA) and stored in diethyl pyrocarbonate (DEPC) H₂O at -20 °C. cDNA was synthesized from total RNA using the RevertAid First Strand cDNA Synthesis Kit (Thermo Fisher Scientific, USA), and 2 μ g cDNA was amplified by qPCR. Next, the levels of multiple mRNAs, as indicated in the corresponding figures, were analyzed by qPCR using the primers shown in the Supplemental Table S2. The relative amount of each mRNA was calculated after normalization to the corresponding 18S mRNA, and the results were expressed as fold change relative to the control group.

2.11. Western blot

Western blot analyses were performed as previously described [15]. Primary antibodies against the following proteins were used: UCP1 (Abcam, ab155117, 1:1000), *PGC1 α* (Abcam, ab54481, 1:1000), *VCAM-1* (Abcam, 134047, 1:1000), *BMP4* (Millipore, MAB1049, 1:1000), β -tubulin (ProteinTech Group, 66240-1-Ig, 1 : 10000), phospho- $\text{I}\kappa\text{B}\alpha$ (Cell Signaling, 2859, 1:1000), $\text{I}\kappa\text{B}\alpha$ (Cell Signaling, 4814, 1:1000), phospho-p65 (Cell Signaling, 3033, 1:1000), p65 (Cell Signaling, 8242, 1:1000), *FASN* (ProteinTech Group, 10624-2-AP, 1 : 1000), *SCD1* (Cell Signaling, 2794, 1:1000), *ATGL* (Cell Signaling, 2138, 1:1000) and *HSL* (Santa Cruz, sc-74489, 1:1000).

2.12. Histological analysis

Immunohistochemistry was performed using a rabbit ABC Staining System (Vector Laboratories, Burlingame, CA, USA) according to the protocol provided by the manufacturer. Briefly, paraffin embedded sections were deparaffinized, rehydrated, microwaved in 0.01 mol/L citrate buffer for 30 min for antigen retrieval, and incubated in 3% hydrogen peroxide for 15 min to quench endogenous peroxidase. Sections were further incubated in 1.5% blocking serum in PBS overnight and then incubated with a rabbit anti-UCP1 or anti-F4/80 monoclonal antibody for 30 min at room temperature, followed with a biotinylated secondary antibody for 30 min at room temperature and AB enzyme reagent for 30 min. Thereafter, the sections were incubated with 150 μ l of peroxidase substrate for 45 s, mounted, and observed under a microscope. For immunofluorescence analysis, anti-UCP1 (Abcam, ab155117, 1:100), and anti-F4/80 (Abcam, ab6640, 1:100) were applied.

2.13. ELISA

IL-1 β levels in mice plasma were quantitated using an ELISA kits (Catalog# ELM-ILb, RayBiotech, USA) according to the manufacturer's instructions.

2.14. Assessment of aortic atherosclerotic lesion areas

Mouse aortas were perfused with PBS followed by 10% formalin or 4% paraformaldehyde. The aortas were pinned on a black wax pan and stained with Oil Red O. Images of the aorta were captured with camera (Catalog#MH-24, Nikon, Japan). Images were analyzed using Image Pro Plus software. For histological analysis of atherosclerotic lesions in the aortic sinus, hearts in the atrioventricular valve region were embedded in OCT for frozen sectioning, and serial 5- μ m-thick sections were stained with Oil Red O.

2.15. Plasma parameters and lipoprotein profiles

Mice were fasted overnight, and blood samples were collected by retroorbital bleeding methods. Sera were prepared and used for measurements. Total triglycerides (TG), total cholesterol (TC), low-density lipoprotein-cholesterol (LDL-C) and high-density lipoprotein-cholesterol (HDL-C) levels were determined using the Sysmex Chemix-180 automatic biochemical analysis device (Sysmex Infosystems).

2.16. Statistical analysis

All data are shown as the mean \pm SEM. GraphPad Prism 8.0 software (GraphPad Software, San Diego, CA, USA) was used to present the data. Statistical comparisons between two groups were performed by unpaired Student's *t*-test, and comparisons among groups of three or more were performed by analysis of variance (ANOVA). Groups were

considered significantly different if P values were <0.05 . Pearson's correlations between BMP4, brown-related genes and white-related genes were calculated. The numbers per group in the figure legends refer to the number of mice per group.

3. Results

3.1. BMP4 expression is decreased in perivascular adipose tissue from mice and humans with atherosclerosis

Two types of adipose tissue exist in humans and mammals: white (inguinal and gonadal) and brown (interscapular and perivascular) adipose tissue. BMP4 has a dual function in adipose tissue by inducing a white-to-brown change in WAT while inhibiting the acquisition of a brown phenotype in brown adipocytes. However, its role in PVAT during the development of atherosclerosis is still undefined. Therefore, to

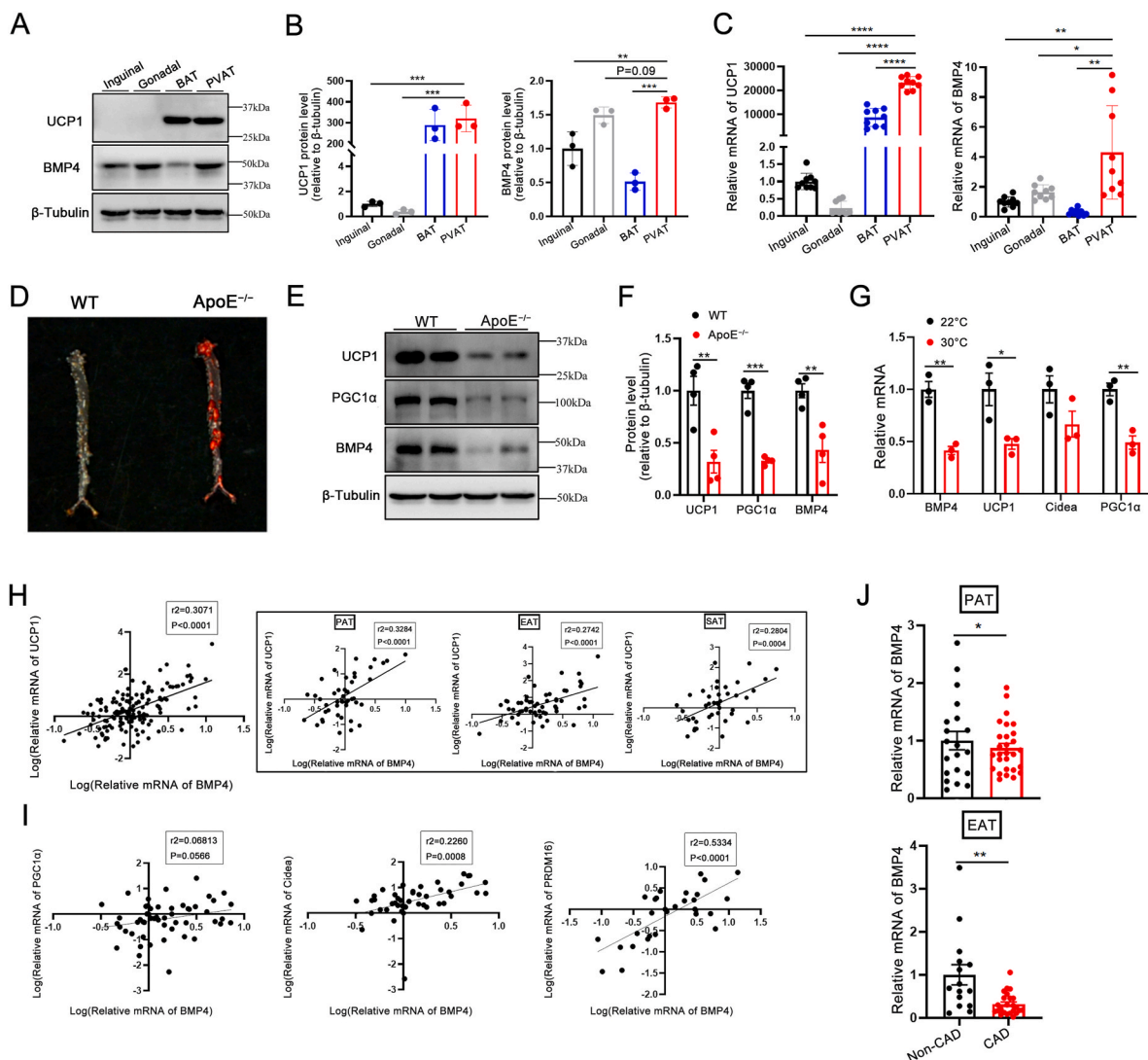


Fig. 1. Interaction between BMP4, PVAT metabolism and CAD. (A) Western blot analysis and quantification (B) of UCP1 and BMP4 expression in different adipose tissues ($n = 3$). (C) Relative mRNA levels of UCP1 and BMP4 were measured by qPCR. ($n = 9$). (D) Representative images corresponding to en face Oil Red O staining of the atherosclerotic lesion of whole aortas from WT and ApoE^{-/-} mice. (E) Western blot analysis and quantification (F) of UCP1, PGC1 α and BMP4 in PVAT of WT or ApoE^{-/-} mice. (G) Relative mRNA levels of BMP4, UCP1, Cidea and PGC1 α were measured by qPCR. ($n = 3$). (H) Correlation analysis of co-expression of BMP4 and UCP1 in human SAT, EAT and PAT. (I) Correlation analysis of co-expression of BMP4 and brown-related genes (PGC1 α , Cidea, PRDM16) in human SAT, EAT and PAT. (J) Relative mRNA levels of BMP4 were determined in PAT and EAT of patients with coronary artery diseases (CAD) or those without. Values are means \pm S.E.M. * $P < 0.05$, ** $P < 0.01$, *** $P < 0.001$ by unpaired Student's *t*-test (F, G and J) or one-way analysis of variance (ANOVA) (B and C). Pearson's correlations between BMP4, and brown-related genes were calculated. (For interpretation of the references to colour in this figure legend, the reader is referred to the Web version of this article.)

answer this question, we first examined the expression of BMP4 in PVAT under physiological and pathological conditions. Our results showed that BMP4 was expressed in different adipose depots with the highest level in PVAT, which was approximately 1.5-fold (protein level) protein

level and 4-fold (mRNA level) higher than inguinal WAT (iWAT). (Fig. 1A-C). Next, we examined BMP4 expression in PVAT from mice with atherosclerosis. We fed wild type (WT) and ApoE^{-/-} mice with western diet (WD) for 21 weeks (Figs. S1A and S1B). The results

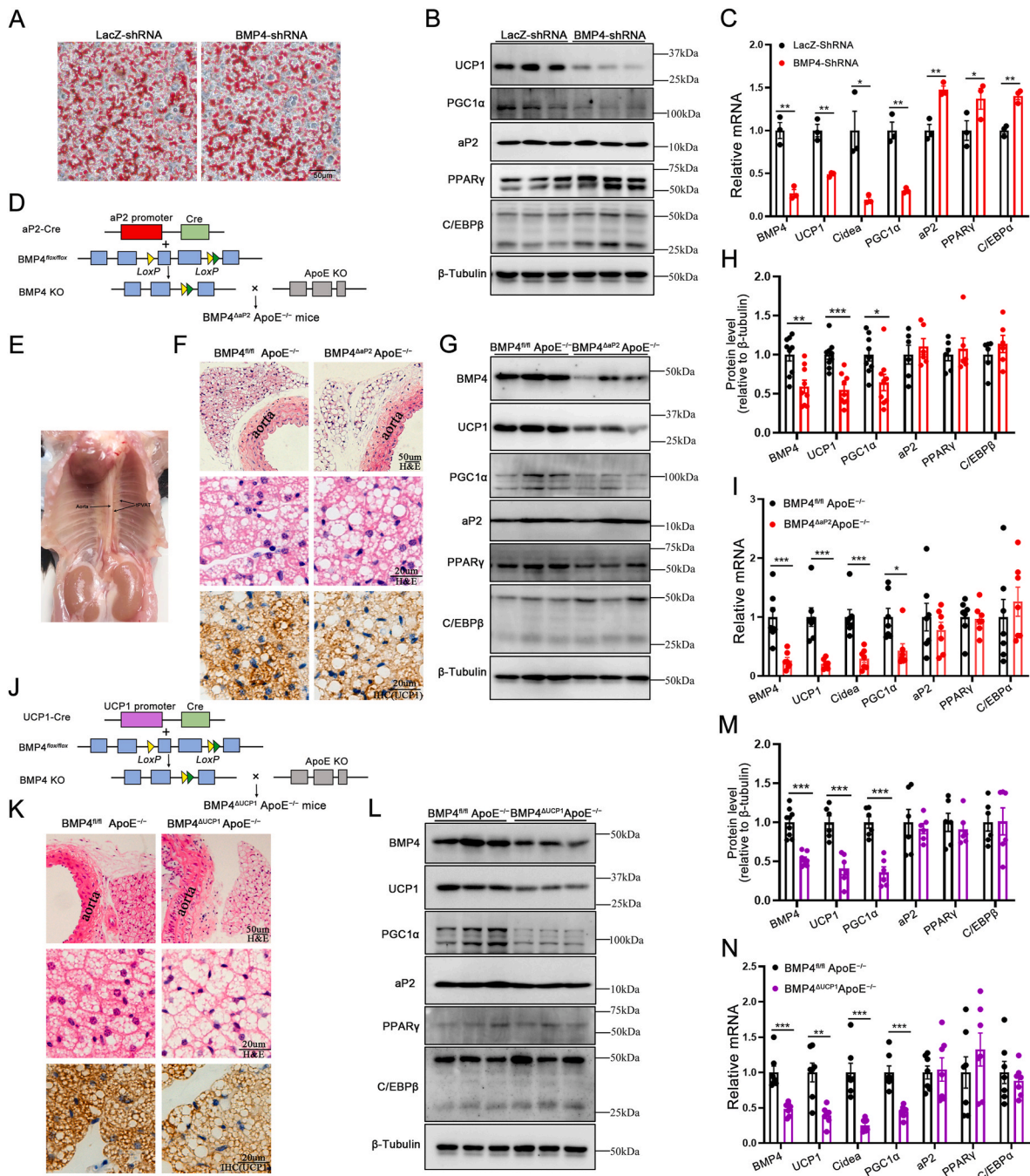


Fig. 2. Absence of BMP4 in PVAT produces a white-like phenotype. (A) Oil Red O staining of adipocytes differentiated from brown preadipocytes on day 8. (B) Western blot analysis of UCP1, Cidea, PGC1 α , aP2, PPAR γ and C/EBP β in brown adipocytes with LacZ knockdown or BMP4 knockdown. (C) Relative mRNA levels of BMP4, UCP1, Cidea, PGC1 α , aP2, PPAR γ and C/EBP α in brown adipocytes with LacZ knockdown or BMP4 knockdown. (D) Schema of FABP4/aP2-Cre-BMP4^{lox/lox} mouse models. (E) Gross picture of adult mouse thoracic aortic PVAT. (F) Representative HE and IHC(UCP1) microscopic picture of PVAT isolated from BMP4^{fl/fl} ApoE^{-/-} and BMP4 ^{Δ aP2} ApoE^{-/-} mice fed with WD for 16 weeks. (G) Western blot analysis and quantification (H) of BMP4, UCP1, PGC1 α , aP2, PPAR γ and C/EBP β in PVAT of BMP4^{fl/fl} ApoE^{-/-} and BMP4 ^{Δ aP2} ApoE^{-/-} mice fed with WD for 16 weeks (n = 6–9). (I) Relative mRNA levels of BMP4, UCP1, Cidea, PGC1 α , aP2, PPAR γ and C/EBP α in PVAT of BMP4^{fl/fl} ApoE^{-/-} and BMP4 ^{Δ aP2} ApoE^{-/-} mice fed with WD for 16 weeks (n = 7). (J) Schema of UCP1-Cre-BMP4^{lox/lox} mouse models. (K) Representative HE and IHC(UCP1) microscopic picture of PVAT isolated from BMP4^{fl/fl} ApoE^{-/-} and BMP4 ^{Δ UCP1} ApoE^{-/-} mice fed with WD for 16 weeks. (L) Western blot analysis and quantification (M) of BMP4, UCP1, Cidea, PGC1 α , aP2, PPAR γ and C/EBP β in PVAT of BMP4^{fl/fl} ApoE^{-/-} and BMP4 ^{Δ UCP1} ApoE^{-/-} mice fed with WD for 16 weeks (n = 6–9). (N) Relative mRNA levels of BMP4, UCP1, Cidea, PGC1 α , aP2, PPAR γ and C/EBP α in PVAT of BMP4^{fl/fl} ApoE^{-/-} and BMP4 ^{Δ UCP1} ApoE^{-/-} mice fed with WD for 16 weeks (n = 7). Values are means \pm S.E.M. *P < 0.05, **P < 0.01, ***P < 0.001 by unpaired Student's *t*-test (C, H, I, M and N). (For interpretation of the references to colour in this figure legend, the reader is referred to the Web version of this article.)

demonstrated that ApoE^{-/-} mice exhibited greater atherosclerotic lesions in the whole aorta than the WT mice (Fig. 1D). Notably, the expression of BMP4, UCP1 and PGC1 α was significantly decreased in PVAT of ApoE^{-/-} mice (Fig. 1E and F). Previous studies have demonstrated that mice housed in thermoneutral conditions, displayed significant adipose tissue inflammation and atherosclerosis development [24]. Therefore, we housed wild-type mice at 22 °C or 30 °C for 3 weeks and examined the changes in the expression of BMP4 and brown-related genes in PVAT. We observed that the PVAT of mice housed at 30 °C displayed less mRNA expression in BMP4 and brown-related genes than the PVAT of mice housed at 22 °C (Fig. 1G). These results are in agreement with our previous work, which showed that the expression of UCP1 and brown-related proteins was lower in pericardial fat from patients with CAD than from those without [15].

Given that the level of BMP4 in human WAT is inversely correlated with BMI [20], we collected paracardial adipose tissue (PAT), epicardial adipose tissue (EAT) and subcutaneous adipose tissue (SAT) from patients with and without coronary heart disease (CAD) undergoing valvular heart surgery for the following study. As shown in Supplementary Table S1, CAD patients were older than those without CAD, and women had a lower incidence of development CAD. In addition, we observed that CAD patients have larger waist size and more likely to have a history of hypertension. Next, we examined the expression level of BMP4 along with some brown and white-related genes. Correlation analysis indicates that the expression of BMP4 in different types of human adipose tissues was positively correlated with the expression of UCP1 and other brown-related genes (Fig. 1H and I), but not with the expression of white-related genes (Fig. S2A). In addition, the expression of BMP4 in human pericardial adipose tissue (PAT and EAT) was decreased in patients with CAD compared with those without (Fig. 1J). Taken together, these results indicate that the brown adipose characteristics of PVAT are closely associated with BMP4 expression, and decreased in vascular diseases.

3.2. Absence of BMP4 in PVAT produces a white-like phenotype

To explore whether BMP4 has a regulatory effect on the browning of PVAT, BMP4 was knocked down in immortalized brown preadipocytes with a BMP4 shRNA. Oil Red O staining showed that BMP4 knockdown had no influence on the adipogenic differentiation of brown adipocytes (Fig. 2A). However, knockdown of BMP4 resulted in a reduced expression of brown-related genes (UCP1, Cidea, PGC1 α) and slightly increased expression of white-related genes (α 2, PPAR γ , C/EBP α , C/EBP β) (Fig. 2B and C). To further explore the roles of BMP4 in PVAT in vivo, we generated two transgenic mouse models with BMP4 and ApoE double knockout (BMP4-KO), by crossing adipocyte-specific BMP4-null (BMP4 ^{Δ ap2}) [20] mice and UCP1-specific BMP4-null (BMP4 ^{Δ UCP1}) mice with ApoE^{-/-} mice (Fig. 2D and J). After feeding on a WD for 16 weeks, there was no significant difference in body weight and food intake between BMP4 ^{Δ ap2} ApoE^{-/-} and BMP4 ^{Δ UCP1} ApoE^{-/-} mice (Figs. S3B–S3C). We isolated thoracic aortic PVAT from BMP4-KO and the control mice for the following study (Fig. 2E). BMP4 ^{Δ ap2} ApoE^{-/-} mice demonstrated a significant reduction, but not total ablation, of BMP4 mRNA and protein expression compared with the BMP4 ^{Δ UCP1} ApoE^{-/-} mice (Fig. 2G–I). Moreover, hematoxylin and eosin (H&E) staining showed dramatic morphological changes in perivascular adipocytes of BMP4 ^{Δ ap2} ApoE^{-/-} mice, including larger adipocyte size and less multilocular lipid droplets as compared with BMP4 ^{Δ UCP1} ApoE^{-/-} mice (Fig. 2F). In addition, immunohistochemical analysis demonstrated lower expression levels of UCP1 in PVAT of BMP4 ^{Δ ap2} ApoE^{-/-} mice compared with BMP4 ^{Δ UCP1} ApoE^{-/-} mice (Fig. 2F). Using quantitative PCR and Western blot, we further confirmed that the expression of UCP1, Cidea and PGC1 α was down-regulated in PVAT of BMP4 ^{Δ ap2} ApoE^{-/-} mice, whereas we observed no significant changes in the expression of white-related genes (Fig. 2G–I). Considering PVAT owns brown-like characteristics, to confirm the function of BMP4 on PVAT

metabolism, more selective UCP1-cre-driven brown adipocyte-specific knockout models were developed (Fig. 2J). After feeding on a WD for 16 weeks, there was no significant difference in body weight and food intake between BMP4 ^{Δ UCP1} ApoE^{-/-} and BMP4 ^{Δ UCP1} ApoE^{-/-} mice (data not shown). Consistently, BMP4 ^{Δ UCP1} ApoE^{-/-} mice showed larger adipocyte size and lower expression levels of UCP1 than BMP4 ^{Δ UCP1} ApoE^{-/-} mice (Fig. 2K). In addition, BMP4 ^{Δ UCP1} ApoE^{-/-} mice showed reduced expression of brown-related genes compared with BMP4 ^{Δ UCP1} ApoE^{-/-} mice (Fig. 2L–N). These data suggest that the knockout of BMP4 in adipose tissue disrupted the metabolism of PVAT and promoted a shift toward a white-like adipocyte phenotype in PVAT.

3.3. Absence of BMP4 in PVAT decreases the fatty acid metabolism

To understand the molecular mechanism that underlies the brown to white-like adipocyte shift in PVAT of BMP4-KO mice, we performed RNA sequencing for detailed analysis of the genome-wide gene expression profile in PVAT from BMP4 ^{Δ ap2} ApoE^{-/-} and BMP4 ^{Δ UCP1} ApoE^{-/-} mice. BMP4 knockout altered the expression of 1628 differentially expressed genes, of which 1218 genes were up-regulated and 410 genes were down-regulated (Fig. 3A and B). Functional annotation using the Gene Ontology database showed that most of the down-regulated genes were involved in metabolism, especially lipid metabolism (Fig. 3C). Moreover, several lipid metabolism-related genes, including MGLL, CPT2, ACAD11, ACS2, PDK4, ACC, FASN, THEM5, SCD1, had reduced expression in the PVAT of BMP4-KO mice (Fig. 3D). Consistent with alterations in the genetic profile, decreased expression of several key lipid metabolism-related genes was validated by qPCR analysis (Fig. 3E). To further validate the function of BMP4 on lipid metabolism of PVAT, we isolated PVAT from BMP4 ^{Δ ap2} ApoE^{-/-} and BMP4 ^{Δ UCP1} ApoE^{-/-} mice and examined the expression levels of genes associated with lipogenesis (FASN and SCD1) and lipolysis (HSL and ATGL). As shown in Fig. 3F–I, deficiency of BMP4 dramatically decreased the expression of the genes. Constantly, qPCR and Western blot analysis showed that knockdown of BMP4 in mature brown adipocytes drastically reduced the expression of genes associated with lipogenesis and lipolysis (Fig. 3J and K). In summary, these data illustrate that BMP4 knockout in PVAT leads to impaired PVAT metabolism, suggesting a potential role for BMP4 in regulating PVAT function during the progression of atherosclerosis.

3.4. BMP4 knockout adipocytes increase endothelial inflammation in vitro

Metabolic dysfunction in PVAT has not yet been considered in the clinical definition of atherosclerosis [25]. The considerable alteration of gene expression involved in lipid metabolism in BMP4-knockout PVAT prompted us to explore the effects on blood vessels. Inflammation is one of the primary causal factors of atherosclerosis. Blood vessels are composed of intimal endothelial cells, media smooth muscle cells and adventitia fibroblasts, all of which play important roles in vascular function [26]. Thus, we tested the response of human umbilical vein endothelial cells (HUVECs), C2C12 myoblasts and human dermal fibroblasts (HDFs) to inflammatory stimuli TNF α . Our results demonstrated that the expression of inflammatory factors was higher in HUVECs than C2C12 myoblasts and HDFs (Fig. S4A), and that exposure to TNF α resulted in increased expression of MCP1, IL-6 in HUVECs. These data suggested that intimal endothelial cells may be the most sensitive cell type to inflammation. Therefore, we focused on the inflammatory response of HUVECs in the remainder of the study.

To establish the inflammatory effects of brown adipocyte on HUVECs, we first incubated HUVECs with conditioned medium obtained from brown adipocytes with BMP4 knockdown (Fig. 4A). qPCR analysis revealed that the mRNA expression of proinflammatory genes (VCAM-1, ICAM-1, MCP1, IL-6 and IL-1 β) was increased by ~2–30-fold in HUVECs incubated with conditioned medium obtained from brown adipocytes

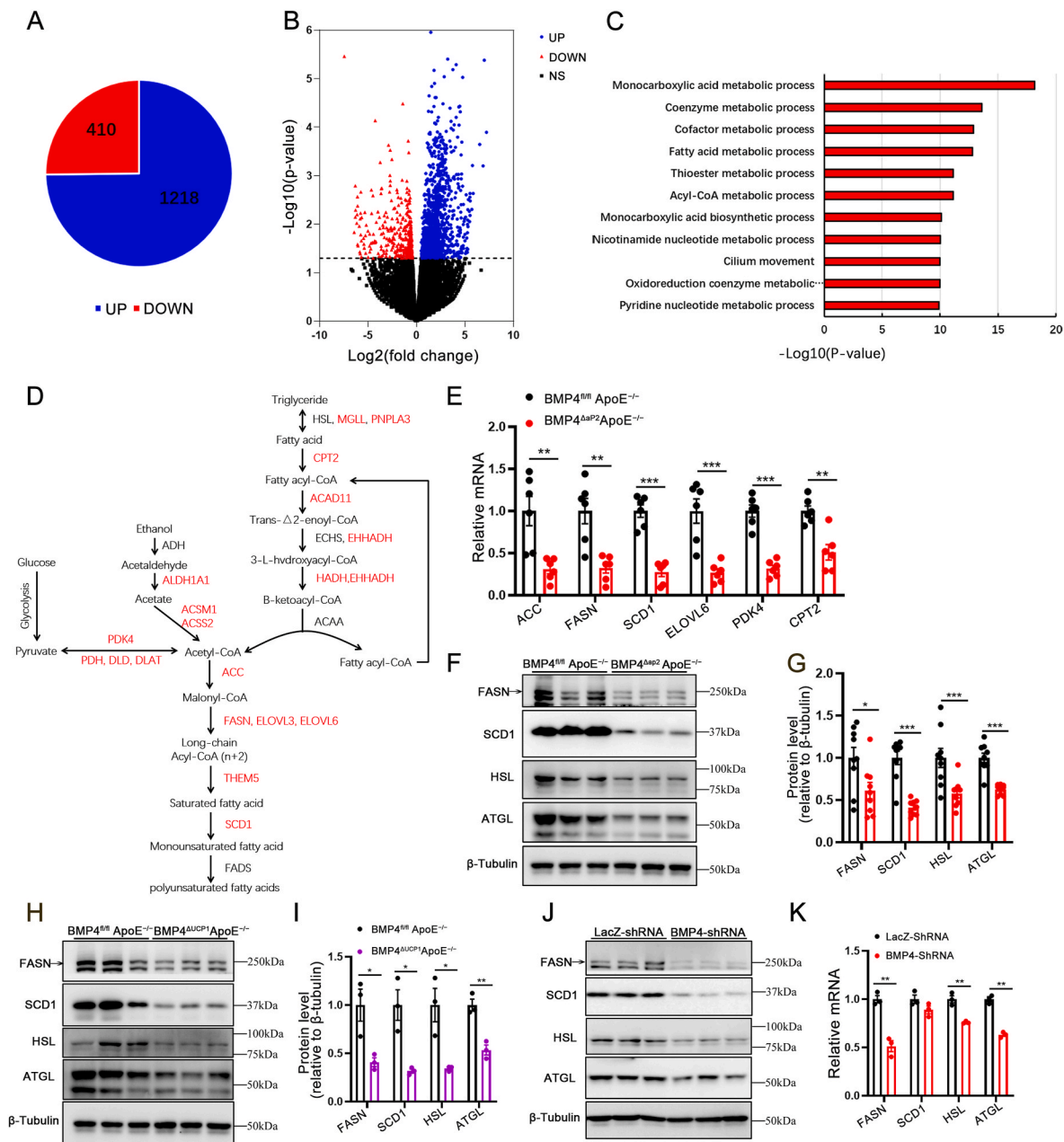


Fig. 3. Absence of BMP4 in PVAT decreases the fatty acid metabolism. (A) Pie graph of RNA sequencing comparing PVAT of $BMP4^{fl/fl} ApoE^{-/-}$ with $BMP4^{\Delta ap2} ApoE^{-/-}$ mice. (B) Volcano plot of RNA sequencing comparing PVAT of $BMP4^{fl/fl} ApoE^{-/-}$ with $BMP4^{\Delta ap2} ApoE^{-/-}$ mice. (C) Gene ontology analysis for down-regulated genes in KEGG pathways, pathways with p value < 0.00015 were listed. (D) Down-regulated genes in PVAT of $BMP4^{\Delta ap2} ApoE^{-/-}$ mice identified by RNA sequencing are marked in red. (E) qPCR validation of genes selected from the pathways in (D). (F) Western blot analysis and quantification (G) of FASN, SCD1, HSL and ATGL in PVAT of $BMP4^{fl/fl} ApoE^{-/-}$ and $BMP4^{\Delta ap2} ApoE^{-/-}$ mice fed with WD for 16 weeks (n = 9). (H) Western blot analysis and quantification (I) of FASN, SCD1, HSL and ATGL in PVAT of $BMP4^{fl/fl} ApoE^{-/-}$ and $BMP4^{\Delta UCP1} ApoE^{-/-}$ mice fed with WD for 16 weeks (n = 3). (J) Western blot analysis of FASN, SCD1, HSL and ATGL in brown adipocytes with LacZ knockdown or BMP4 knockdown. (K) Relative mRNA levels of FASN, SCD1, HSL and ATGL in brown adipocytes with LacZ knockdown or BMP4 knockdown. Values are means \pm S.E.M. *P < 0.05, **P < 0.01, ***P < 0.001 by unpaired Student's t-test (E, G, I, and K). (For interpretation of the references to colour in this figure legend, the reader is referred to the Web version of this article.)

with BMP4 knockdown, compared with cells incubated with the control conditioned medium (Fig. 4B). In addition, Western blot analysis suggested that HUVECs incubated with conditioned medium obtained from brown adipocytes with BMP4 knockdown increased protein expression level of VCAM-1 (Fig. 4C). To explore whether adipocytes with BMP4 overexpression have an effect of improving HUVEC inflammation, we incubated HUVECs with conditioned medium obtained from brown adipocytes with BMP4 overexpression (Fig. 4D). The results showed that the mRNA expression of proinflammatory genes was reduced by ~30–70% in HUVECs with conditioned medium obtained from brown

adipocyte with BMP4 overexpression compared with the controls (Fig. 4E). Moreover, Western blot analysis demonstrated lower expression of VCAM-1 in HUVECs with conditioned medium obtained from brown adipocyte with BMP4 overexpression than the controls (Fig. 4F).

Given the metabolic differences between WAT and BAT, which may influence the function of HUVECs differently, we co-cultured different adipose tissues with HUVECs pretreated with TNF α in a transwell system (Fig. 4G). The mRNA level of the proinflammatory genes *VCAM-1*, *ICAM-1*, *MCPI*, *IL-6* and *IL-1 β* , was lower in HUVECs co-cultured with BAT and PVAT (Fig. S4B). We also observed that PVAT of $ApoE^{-/-}$ mice

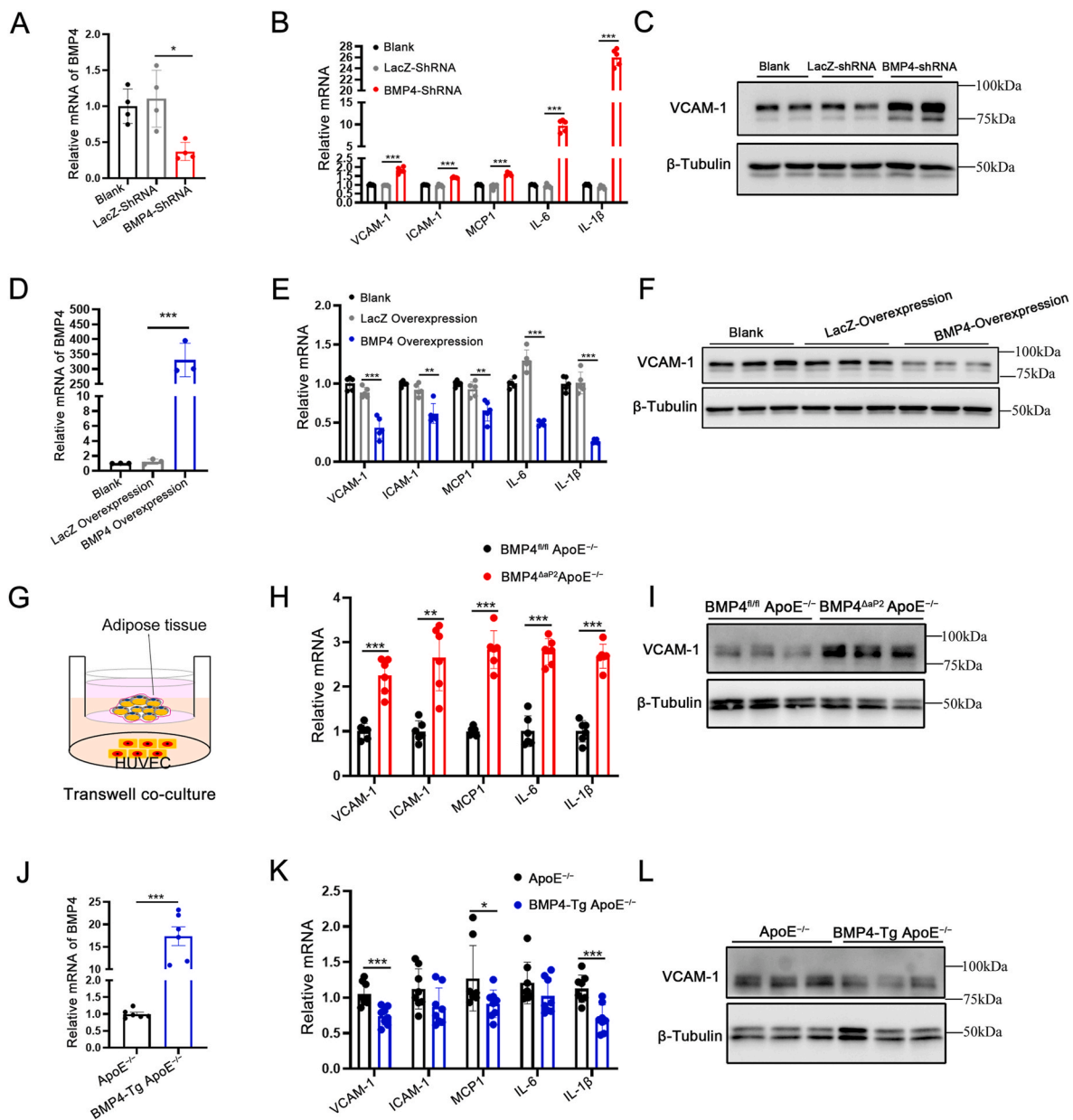


Fig. 4. BMP4 knockout adipocyte increase endothelial inflammation in vitro. (A) Relative mRNA levels of BMP4 in brown adipocytes with BMP4 knockdown and the controls. (B) Relative mRNA levels of VCAM-1, ICAM-1, MCP1, IL-6 and IL1 β in TNF α pretreated HUVECs incubated with conditioned medium from brown adipocytes with BMP4 knockdown and the controls. (C) Western blot analysis of VCAM-1 expression in TNF α pre-treated HUVECs incubated with conditioned medium from brown adipocytes with BMP4 knockdown and the controls. (D) Relative mRNA expression levels of BMP4 in brown adipocytes with BMP4 overexpression and the controls. (E) Relative mRNA levels of VCAM-1, ICAM-1, MCP1, IL-6 and IL1 β in TNF α pre-treated HUVECs incubated with conditioned medium from brown adipocytes with BMP4 overexpression and the controls. (F) Western blot analysis of VCAM-1 expression in TNF α pre-treated HUVECs incubated with conditioned medium from brown adipocytes with BMP4 overexpression and the controls. (G) Schematic of the transwell coculture chamber. (H) Relative mRNA levels of VCAM-1, ICAM-1, MCP1, IL-6 and IL1 β in TNF α pre-treated HUVECs that were co-cultured for 24 h with PVAT isolated from BMP4^{fl/fl} ApoE^{-/-} and BMP4 ^{Δ ap2} ApoE^{-/-} mice fed with WD for 16 weeks (n = 6). (I) Western blot analysis of VCAM-1 in TNF α pre-treated HUVECs that were co-cultured for 24 h with PVAT isolated from BMP4^{fl/fl} ApoE^{-/-} and BMP4 ^{Δ ap2} ApoE^{-/-} mice fed with WD for 16 weeks (n = 3). (J) Relative mRNA levels of BMP4 in PVAT of BMP4^{fl/fl} ApoE^{-/-} and BMP4 ^{Δ ap2} ApoE^{-/-} mice fed with WD for 20 weeks (n = 6). (K) Relative mRNA levels of VCAM-1, ICAM-1, MCP1, IL-6 and IL1 β in TNF α pre-treated HUVECs that were co-cultured for 24 h with PVAT isolated from ApoE^{-/-} and BMP4-Tg ApoE^{-/-} mice fed with WD for 20 weeks (n = 6). (L) Western blot analysis of VCAM-1 expression in TNF α pre-treated HUVECs that were co-cultured for 24 h with PVAT isolated from ApoE^{-/-} and BMP4-Tg ApoE^{-/-} mice fed with WD for 20 weeks (n = 3). Values are means \pm S.E.M. *P < 0.05, **P < 0.01, ***P < 0.001 by unpaired Student's *t*-test (H, J and K) or one-way analysis of variance (ANOVA) (A and B, D and E). (For interpretation of the references to colour in this figure legend, the reader is referred to the Web version of this article.)

increased proinflammatory gene expression in TNF α -pretreated HUVECs compared with the WT mice. In addition, PVAT of old ApoE^{-/-} mice showed more severe proinflammatory capability than young ApoE^{-/-} mice (Figs. S4C and S4D). These data indicate that the metabolic activity of adipose tissue is positively related to its anti-inflammatory activity.

To investigate whether BMP4-mediated activation of PVAT

metabolism promotes anti-inflammatory activity, we co-cultured PVAT from BMP4 ^{Δ ap2} ApoE^{-/-} and BMP4^{fl/fl} ApoE^{-/-} mice with TNF α pre-treated HUVECs and investigated changes in proinflammatory gene expression. The PVAT from BMP4 ^{Δ ap2} ApoE^{-/-} mice induced expression of proinflammatory molecules, generally with a 2–3-fold increase in mRNA levels (Fig. 4H). Similarly, the protein level of VCAM-1 was

drastically increased in HUVECs co-cultured with PVAT from BMP4^{Δap2} ApoE^{-/-} mice compared to the controls (Fig. 4I). Next, we generated ApoE^{-/-} mice with adipocyte specific overexpression of BMP4 (BMP4-Tg ApoE^{-/-}) driven by the ap2 promoter. PVAT derived from BMP4-Tg ApoE^{-/-} mice displayed markedly increased BMP4 mRNA expression (Fig. 4J). Using a transwell assay, we confirmed that PVAT of BMP4-Tg ApoE^{-/-} mice significantly reduced HUVECs inflammation, as demonstrated by a drastic decline in the mRNA and protein level of proinflammatory genes (Fig. 4K and L).

As a metabolically active endocrine tissue, adipose tissue produces various secreted factors, including BMP4. To understand whether the protective effect of PVAT from BMP4-Tg ApoE^{-/-} mice on HUVEC inflammation is dependent on activation of the PVAT metabolism, we incubated HUVECs with recombinant mouse BMP4 (10, 20 and 40 ng/mL) and examined the expression of proinflammatory genes. BMP4 did not induce proinflammatory gene expression, indicating that BMP4 was not a direct regulator of endothelial cells inflammation (Figs. S4E and S4F).

3.5. BMP4 deficiency accelerates atherosclerotic plaque formation in ApoE^{-/-} mice

Inflammation is recognized as playing a key role in the development of atherosclerosis. Therefore, we explored the pathophysiological roles of adipocyte-derived BMP4 in atherosclerosis. Gross examination by general Oil Red O staining revealed that arteries, including the aorta arch, thoracic artery, abdominal artery, and common iliac artery, contained widespread atherosclerotic plaques throughout the artery stem both in BMP4^{fl/fl} ApoE^{-/-} and BMP4^{Δap2} ApoE^{-/-} mice. Noticeably, the average sizes of plaque areas were larger in arteries of BMP4^{Δap2} ApoE^{-/-} mice, (2.0-fold greater) compared with the littermate ApoE^{-/-} mice (Fig. 5A and B). Furthermore, quantification of lipid deposition in the aortic sinus, via Oil Red O staining, revealed that BMP4^{Δap2} ApoE^{-/-} mice had ~2-fold increase in aortic lipid accumulation and ~3-fold increase in atherosclerotic plaques (Fig. 5C–E). We further confirmed that aortas from BMP4^{Δap2} ApoE^{-/-} mice have high VCAM-1 expression compared with the controls (Fig. 5F and G). These data indicate that BMP4 knockout in adipose tissues promotes the development of vascular inflammation and atherosclerosis. Activation of lipolysis in adipose tissue is likely to alter blood lipid profiles. Indeed, metabolic parameter analysis exhibited a significant increase in plasma total cholesterol (TC) and low-density lipoprotein-cholesterol (LDL-C) in BMP4^{Δap2} ApoE^{-/-} mice (Fig. 5H), suggesting that the reduced metabolic activity of PVAT and other adipose tissues in BMP4^{Δap2} ApoE^{-/-} mice may result in dyslipidemia. In another model, the aorta from BMP4^{ΔUCP1} ApoE^{-/-} mice showed an approximately 2-fold increase of atherosclerotic plaques (Fig. 5I and J). Quantification of Oil Red O staining on the aortic sinus similarly revealed an approximately 2-fold increase in aortic lipid accumulation and a modest increase in atherosclerotic plaques in BMP4^{ΔUCP1} ApoE^{-/-} mice (Fig. 5K–M). Western blot analysis suggested that aortas from BMP4^{ΔUCP1} ApoE^{-/-} mice have a high level of expression of VCAM-1 compared with the controls (Fig. 5N–O). Remarkably, there was no significant difference in TC and LDL-C between BMP4^{ΔUCP1} ApoE^{-/-} and BMP4^{fl/fl} ApoE^{-/-} mice (Figure 5P), suggesting that BMP4 knockout in BAT exacerbates local inflammation in atherosclerotic lesions without influencing systemic lipoprotein composition.

3.6. Overexpression of BMP4 in adipocytes promotes browning of PVAT and inhibits atherosclerosis in ApoE^{-/-} mice

BMP4-Tg ApoE^{-/-} mice were generated to explore whether BMP4 overexpression in brown adipocytes may represent a therapeutic approach to counteract atherosclerosis by inducing browning of PVAT. The body weight and food intake were lower in TG mice on a WD (Figs. S5A–S5C). H&E staining showed that the size of perivascular

adipocytes was reduced in BMP4-Tg ApoE^{-/-} mice, and IHC showed higher expression of UCP1 in the PVAT of BMP4-Tg ApoE^{-/-} compared with the control group (Fig. 6A). These data suggest that BMP4 plays a key role in activating PVAT metabolism. In support of this notion, the mRNA and protein levels of UCP1 and PGC1α were found to be increased in the PVAT of BMP4-Tg ApoE^{-/-} mice (Fig. 6B–D). Additionally, Oil Red O staining of the whole aorta and aortic sinus revealed significantly less plaques in BMP4-Tg ApoE^{-/-} mice than in the controls (Fig. 6E–I), supporting the idea that activation of the PVAT metabolism has a protective effect on atherosclerosis. Furthermore, VCAM-1 expression was reduced in the aortas of BMP4-Tg ApoE^{-/-} mice (Fig. 6J and K). The plasma levels of total triglyceride (TG), cholesterol (TC), low-density lipoprotein-cholesterol (LDL-C) and high-density lipoprotein-cholesterol (HDL-C) showed no significant differences (Figure 6L), suggesting that BMP4 overexpression in brown adipocytes had no clear effect on hypertriglyceridemia and hypercholesterolemia.

Previous studies have suggested that increased BAT or beige adipose tissue accelerates the clearance of plasma lipids and protects against atherosclerosis development [13,27]. To exclude the potential contribution of BAT to the observed reduction in atherosclerosis, we examined BAT metabolic activity in BMP4-Tg ApoE^{-/-} mice and its corresponding control mice. H&E staining and IHC indicated that adipocyte morphologies of BAT with BMP4 overexpression were bigger than the controls (Fig. S5D). Western blot analysis further confirmed that BMP4 overexpression decreases the activation of BAT metabolism (Figs. S5E and S5F). Taken together, these results reveal that overexpression of BMP4 in adipose tissue can activate PVAT metabolism, thereby protecting against the development of vascular inflammation and atherosclerosis.

3.7. BMP4 knockdown in brown adipocytes increases the secretion of proinflammatory factors

We next performed gene ontology (GO) enrichment analysis on the up-regulated genes found by RNA sequencing from BMP4^{Δap2} ApoE^{-/-} mice and BMP4^{fl/fl} ApoE^{-/-} mice. The results of BMP4 knockout in PVAT showed activation of many immune response pathways (Fig. 7A), indicating the proinflammatory function of BMP4 knockout in adipocytes. We selected genes from T cell activation pathway to confirm with qPCR, and the results showed that all the genes were up-regulated in the PVAT of BMP4^{Δap2} ApoE^{-/-} mice compared to the controls (Fig. 7B). Meanwhile, we examined the expression of pro-inflammatory macrophages marker F4/80 in PVAT of BMP4^{Δap2} ApoE^{-/-} mice and BMP4^{ΔUCP1} ApoE^{-/-} mice. We found that PVAT of BMP4^{Δap2} ApoE^{-/-} mice had ~3-fold and PVAT of BMP4^{ΔUCP1} ApoE^{-/-} mice had a ~2.5-fold increase in macrophage infiltration compared with the control mice (Fig. 7C and E). In addition, we observed that the mRNA expression of inflammatory cytokines was dramatically increased, particularly IL-1β, in the PVAT of BMP4^{Δap2} ApoE^{-/-} mice compared with the controls (Fig. 7D). By contrast, the expression of M2 macrophage genes (*Arg1* and *Mrc1*) was not significantly different between BMP4^{Δap2} ApoE^{-/-} and BMP4^{fl/fl} ApoE^{-/-} mice (Fig. 7D). We observed the same phenotype in the PVAT of BMP4^{ΔUCP1} ApoE^{-/-} mice by qPCR analysis (Fig. 7F). Correspondingly, PVAT of BMP-Tg ApoE^{-/-} mice displayed ~75% reduction in macrophage infiltration, and a significant reduction in proinflammatory gene expression compared to the controls (Fig. 7G and H). To explore whether WAT have an effect on atherosclerosis in BMP4^{ΔUCP1} ApoE^{-/-} mice, we examined the mRNA expression of brown-related genes, white-related genes, proinflammatory genes and M2 genes in iWAT and gonadal WAT (gWAT). There were no significant changes in gene expression in iWAT (Fig. S6A); however, the white-related genes ap2, PPARγ, the proinflammatory gene MCP1, and M2 gene *Mrc1* were slightly increased in gWAT (Fig. S6B).

We further performed proteomic analysis to identify candidate proteins mediating the adipocytes effects on HUVEC inflammation (Fig. 7I). We found that the release of several proteins was increased, among them the most significant was CCL2/MCP1 (Fig. 7J). These data suggest that

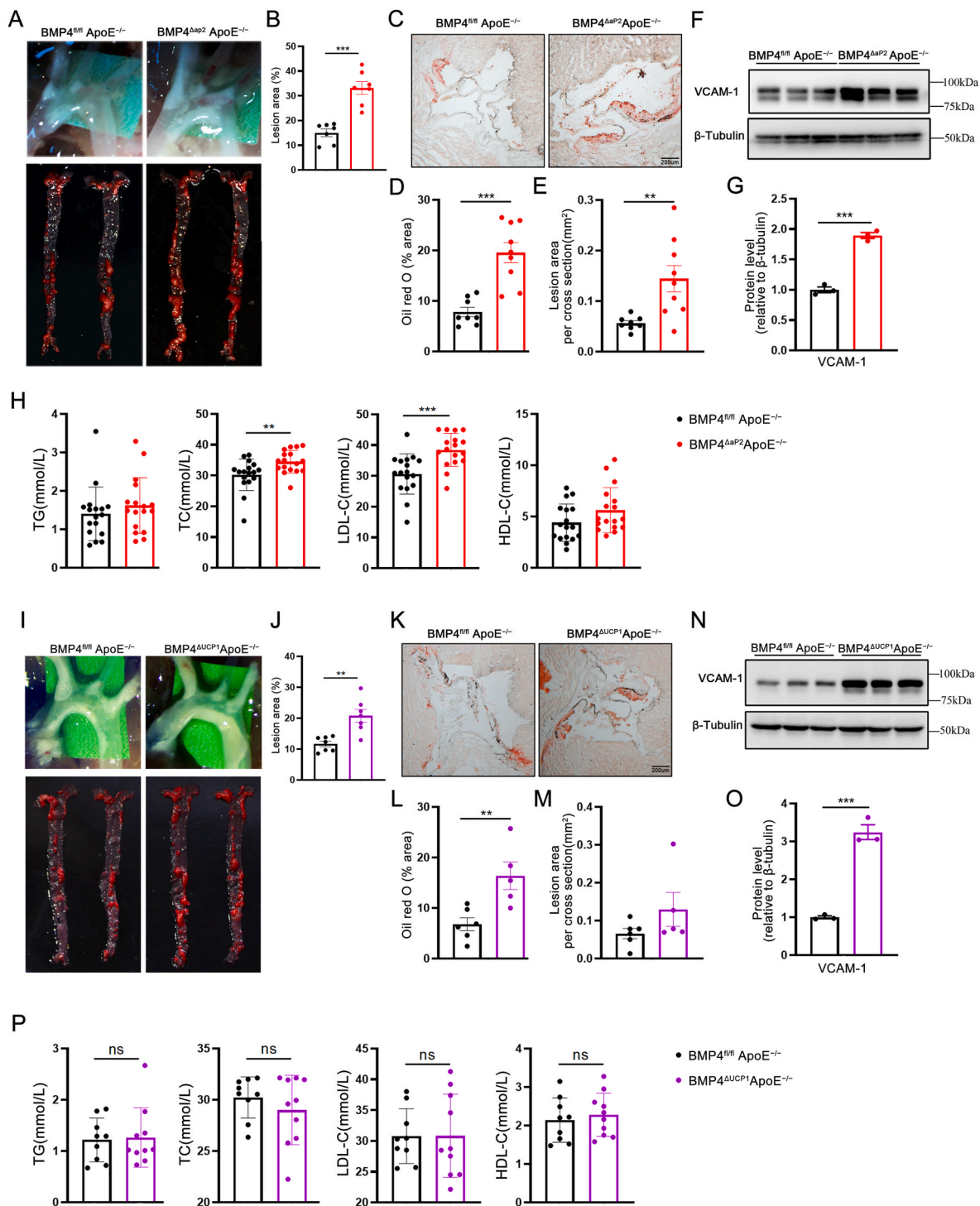


Fig. 5. BMP4 deficiency accelerates atherosclerotic plaque formation in ApoE^{-/-} mice. (A) En face Oil Red O staining of whole aortas from BMP4^{fl/fl} ApoE^{-/-}, BMP4^{Δap2} ApoE^{-/-} mice fed with WD for 16 weeks. (B) Quantification of atherosclerotic lesion size in the whole aortas (n = 7). (C) Representative oil red O staining of cross-sections of aortic sinus. (D) Quantification of positive area for oil red O staining (n = 8–9). (E) Quantification of average lesion size in aortic sinus (n = 8–9). (F) Western blot analysis and quantification (G) of VCAM-1 expression (n = 3). (H) The levels of plasma total triglyceride (TG), cholesterol (TC) and low-density lipoprotein-cholesterol (LDL-C) and high-density lipoprotein-cholesterol (HDL-C) in mice (n = 17). (I) En face Oil Red O staining of whole aortas from BMP4^{fl/fl} ApoE^{-/-}, BMP4^{Δucp1} ApoE^{-/-} mice fed with WD for 16 weeks. (J) Quantification of atherosclerotic lesion size in the whole aortas (n = 7). (K) Representative oil red O staining of cross-sections of aortic sinus. (L) Quantification of positive area for oil red O staining (n = 5–6). (M) Quantification of average lesion size in aortic sinus (n = 5–6). (N) Western blot analysis and quantification (O) of VCAM-1 expression (n = 3). (P) The levels of plasma TG, TC and LDL-C and HDL-C in mice (n = 10). Values are means ± S.E.M. *P < 0.05, **P < 0.01, ***P < 0.001 by unpaired Student's t-test (B, D, E, G, H, J, L, M, N, O and P). (For interpretation of the references to colour in this figure legend, the reader is referred to the Web version of this article.)

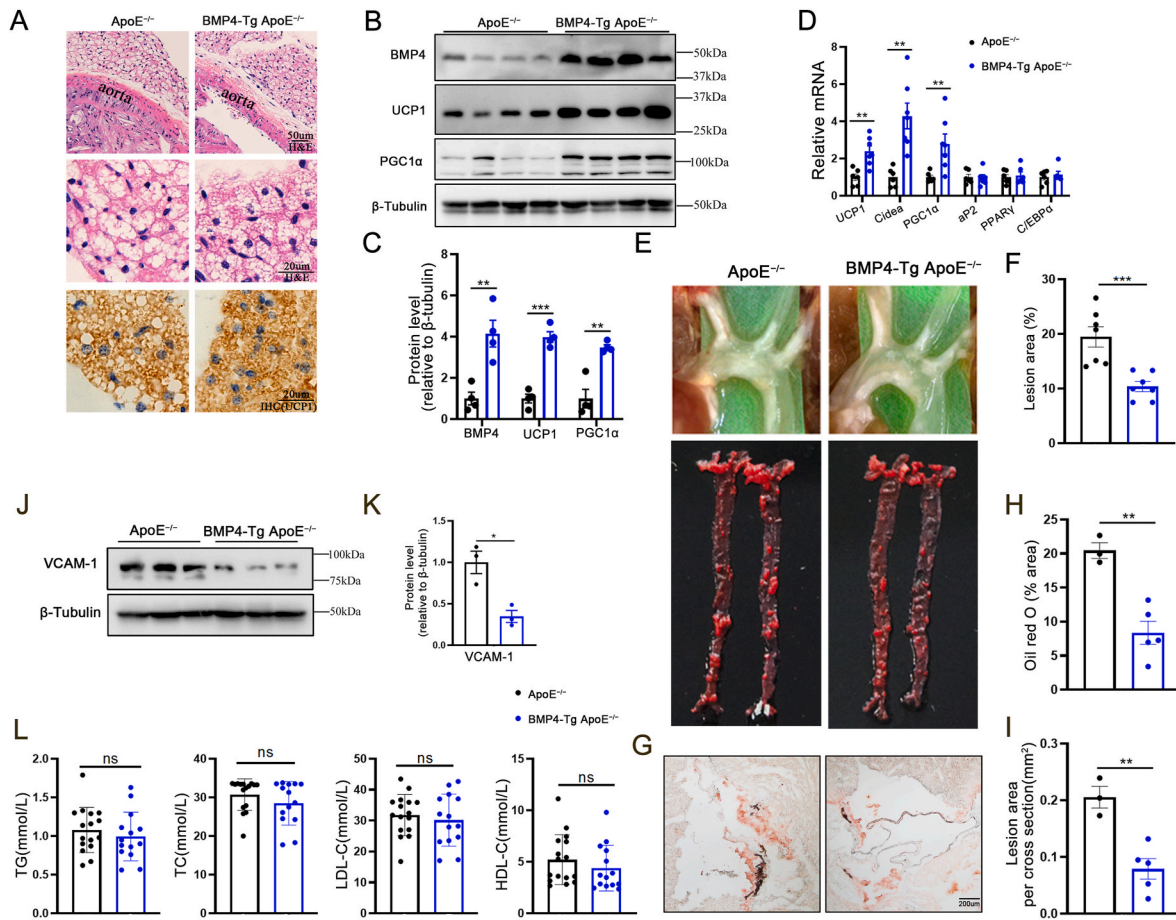


Fig. 6. Overexpression of BMP4 in adipocyte promotes browning of PVAT and inhibits atherosclerosis in $ApoE^{-/-}$ mice. Male $ApoE^{-/-}$ and $BMP4-Tg ApoE^{-/-}$ mice were fed with WD for 20 weeks. (A) Representative HE and IHC(UCP1) microscopic picture of PVAT isolated from $ApoE^{-/-}$ and $BMP4-Tg ApoE^{-/-}$ mice. (B) Western blot analysis and quantification (C) of BMP4, UCP1, PGC1 α , aP2, PPAR γ and C/EBP β in PVAT of $ApoE^{-/-}$ and $BMP4-Tg ApoE^{-/-}$ mice (n = 4). (D) Relative mRNA levels of UCP1, Cidea, PGC1 α , aP2, PPAR γ and C/EBP α in PVAT of $ApoE^{-/-}$ and $BMP4-Tg ApoE^{-/-}$ mice (n = 6). (E) En face Oil Red O staining of whole aortas from $ApoE^{-/-}$ and $BMP4-Tg ApoE^{-/-}$ mice. (F) Quantification of atherosclerotic lesion size in the whole aortas (n = 7). (G) Representative Oil Red O staining of cross-sections of aortic sinus. (H) Quantification of positive area for oil red O staining (n = 3–5). (I) Quantification of average lesion size in aortic sinus (n = 3–5). (J) Western blot analysis and quantification (K) of VCAM-1 expression (n = 3). (L) The levels of plasma TG, TC, LDL-C and HDL-C in mice (n = 14–16). Values are means \pm S.E.M. *P < 0.05, **P < 0.01, ***P < 0.001 by unpaired Student's *t*-test (C, D, F, H, I, K and L). (For interpretation of the references to colour in this figure legend, the reader is referred to the Web version of this article.)

adipocyte-derived proinflammatory factors might initiate the inflammatory response of HUVECs in a paracrine manner. Thus, we examined the level of classical adipocyte-derived proinflammatory factors, including TNF α , IL-1 β , IL-6 and MCP1 in brown adipocytes. We confirmed that *BMP4* knockdown induced adipocyte inflammation, as indicated by the increased expression of proinflammatory factors (Fig. 7K). Moreover, MCP1 had the highest expression compared with the other proinflammatory factors, which may explain why MCP1 was the only cytokine found by proteomics analysis (Figure 7L). To further understand which of these factors is the most important in mediating the inflammatory response, HUVECs were treated with different factors (all 10 ng/mL) or different concentrations according to corresponding expression levels in adipocytes. Western blot analysis suggested that only TNF α and IL-1 β could directly initiate HUVEC inflammation, and that IL-1 β induced more significant inflammation than TNF α in the physiological level (Figure 7M). These data indicated that IL-1 β plays more important role in regulating HUVEC inflammation as an adipocyte-derived factor. The results of quantitative ELISA further confirmed higher IL-1 β levels in conditioned medium from brown adipocytes with *BMP4* knockdown than controls (Figure 7N). However, there was no significant difference in plasma IL-1 β between $BMP4^{\Delta aP2} ApoE^{-/-}$ and $BMP4^{\Delta I/II} ApoE^{-/-}$ mice (Figure 7O). A similar result was observed in

plasma IL-1 β $BMP4^{\Delta UCP1} ApoE^{-/-}$ and $BMP4^{\Delta I/II} ApoE^{-/-}$ mice (Figure 7O). These data suggest that *BMP4* deficiency in perivascular adipocytes increased production of IL-1 β , which contributes to endothelial cells inflammation.

NF- κ B is a key transcription factor governing the expression of most proinflammatory genes. To understand whether *BMP4*-mediated inflammatory responses are dependent on activation of NF- κ B signaling pathway, we examined the expression of proteins involved in NF- κ B signaling pathway when *BMP4* was knocked down. The results show that knockdown of *BMP4* strongly stimulates the phosphorylation of I κ B and p65, and I κ B degradation, which led to translocation of the NF- κ B complex into the nucleus to initiate transcription (Figure 7P). Furthermore, when brown adipocytes were treated with BMS-345541, a highly selective inhibitor of I κ B kinase, *BMP4* knockdown induced phosphorylation of I κ B and p65 was effectively reversed (Figure 7Q), and *BMP4* knockdown induced over-production of proinflammatory factors was decreased (Figure 7R).

3.8. *BMP4* knockdown impairs PGC1 α mediated lipid metabolism in brown adipocytes

We previously showed that, PGC1 α is a key factor in *BMP4*-

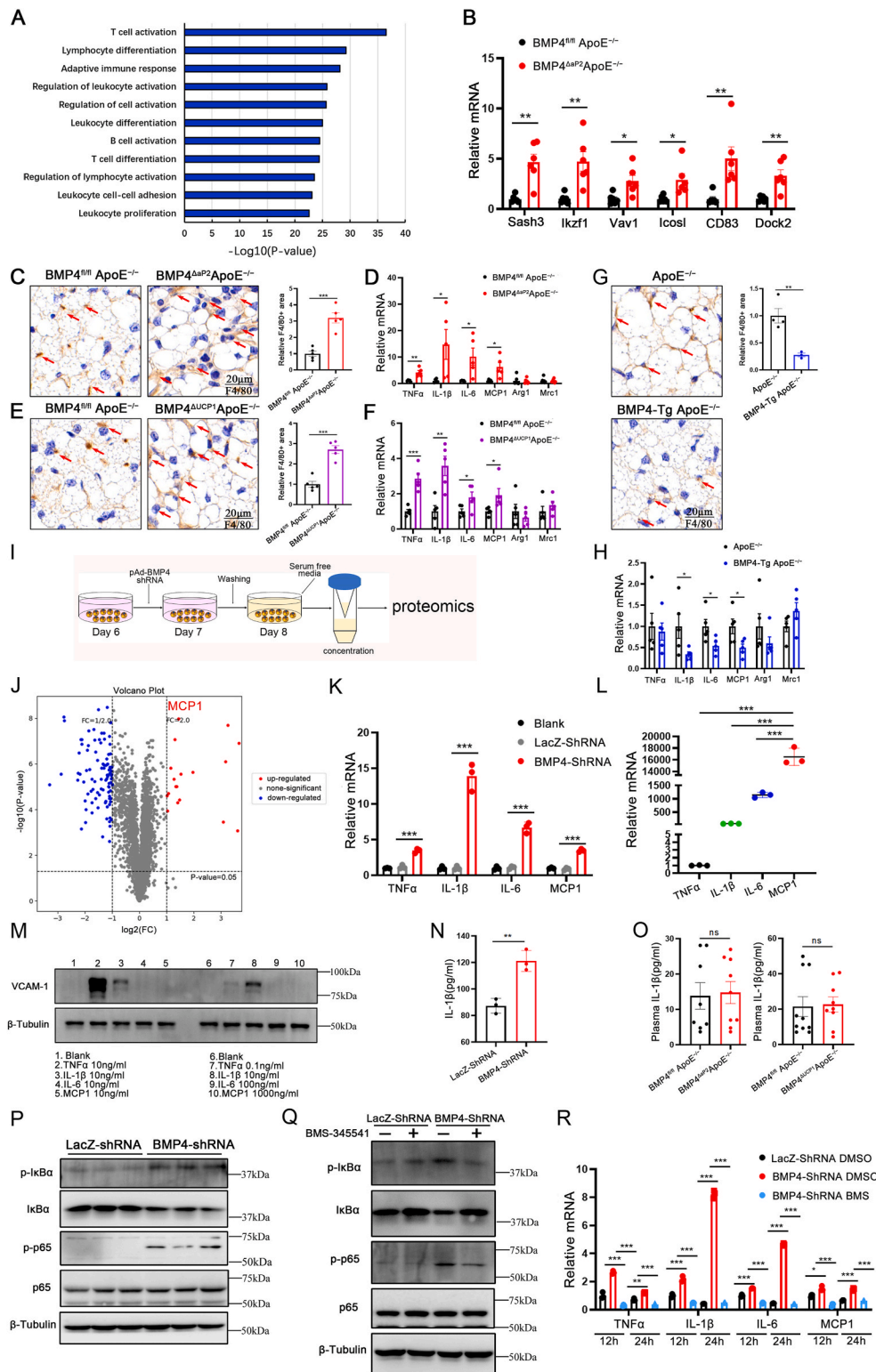


Fig. 7. BMP4 knockdown in brown adipocytes increase adipocyte inflammation and pro-inflammatory factors secretion. (A) Gene ontology analysis for up-regulated genes in KEGG pathways, pathways with p value < 0.00015 were listed. (B) qPCR validation of genes selected from the T cell activation pathways. (C) Immunohistochemical staining of F4/80 expression in PVAT of $BMP4^{fl/fl} ApoE^{-/-}$ and $BMP4^{\Delta aP2} ApoE^{-/-}$ mice. The right graph shows the quantification of F4/80 positive cells in C ($n = 5$). (D) Relative mRNA levels of BMP4, UCP1, Cidea, PGC1 α , aP2, PPAR γ and C/EBP α in PVAT of $BMP4^{fl/fl} ApoE^{-/-}$ and $BMP4^{\Delta aP2} ApoE^{-/-}$ mice fed with WD for 16 weeks ($n = 5$). (E) Immunohistochemical staining of F4/80 expression in PVAT of $BMP4^{fl/fl} ApoE^{-/-}$ and $BMP4^{\Delta UCP1} ApoE^{-/-}$ mice. The right graph shows the quantification of F4/80 positive cells in C ($n = 5$). (F) Relative mRNA levels of BMP4, UCP1, Cidea, PGC1 α , aP2, PPAR γ and C/EBP α in PVAT of $BMP4^{fl/fl} ApoE^{-/-}$ and $BMP4^{\Delta UCP1} ApoE^{-/-}$ mice fed with WD for 16 weeks ($n = 5$). (G) Immunohistochemical staining of F4/80 expression in PVAT of $ApoE^{-/-}$ and $BMP4-Tg ApoE^{-/-}$ mice. The right graph shows the quantification of F4/80 positive cells in C ($n = 3-4$). (H) Relative mRNA levels of BMP4, UCP1, Cidea, PGC1 α , aP2, PPAR γ and C/EBP α in PVAT of $ApoE^{-/-}$ and $BMP4-Tg ApoE^{-/-}$ mice fed with WD for 20 weeks ($n = 5$). (I) Workflow of the collection of brown adipocytes supernatant for proteomic analysis. (J) Volcano plot of adipocyte-conditioned medium proteome comparing BMP4 knockdown with lacZ knockdown. (K) Relative mRNA levels of TNF α , IL1 β , IL-6 and MCP1 in brown adipocytes with BMP4 knockdown or the controls. (L) Corresponding mRNA expression levels of TNF α , IL1 β , IL-6 and MCP1 in brown adipocyte. (M) Western blot analysis of VCAM-1 expression in HUVECs. (N) Levels of the inflammatory cytokines IL1 β in the medium from adipocyte with BMP4 knockdown and LacZ knockdown. (O) Plasma concentrations of IL1 β in WD-fed $BMP4^{fl/fl} ApoE^{-/-}$, $BMP4^{\Delta aP2} ApoE^{-/-}$, and $BMP4^{\Delta UCP1} ApoE^{-/-}$ mice. (P) Western blot analysis of p-IkBa, IkBa, p-p65, and p65 in brown adipocytes with BMP4 knockdown or lacZ knockdown. (Q) Western blot analysis of p-IkBa, IkBa, p-p65, and p65 in brown adipocytes cultured with or without NF- κ B pathway inhibitor BMS-345541. (R) Relative mRNA levels of TNF α , IL1 β , IL-6 and MCP1 in brown adipocytes cultured with or without NF- κ B pathway inhibitor BMS-345541. Values are means \pm S.E.M. * $P < 0.05$, ** $P < 0.01$, *** $P < 0.001$ by unpaired Student's t -test (B to H, N and O), one-way analysis of variance (ANOVA) (K and L) or two-way analysis of variance (ANOVA) (R). (For interpretation of the references to colour in this figure legend, the reader is referred to the Web version of this article.)

medicated browning. To investigate whether PGC1 α exerts its effects on BMP4-mediated adipocytes inflammation, we first examined the PGC1 α protein level when BMP4 was overexpressed in brown adipocytes. As expected, BMP4 overexpression activated PGC1 α expression (Fig. S7A). When BMP4 was knocked down, mRNA expression of PGC1 α , and that of genes involved in lipid metabolism were drastically decreased (Figs. 2G and 3E). To further examine whether BMP4-mediated adipocyte inflammation is dependent on PGC1 α , we

knocked down PGC1 α expression in immortalized brown preadipocytes with a PGC1 α shRNA and examined the impact on proinflammatory gene expression (Fig. 8A). As expected, the expression of proinflammatory genes increased in brown adipocytes with PGC1 α knockdown compared with those in the controls (Fig. 8B), in a pattern similar to that observed in BMP4-knockdown adipocytes (Fig. 7K). Furthermore, we incubated HUVECs with conditioned medium obtained from brown adipocytes with PGC1 α knockdown, and found a significant

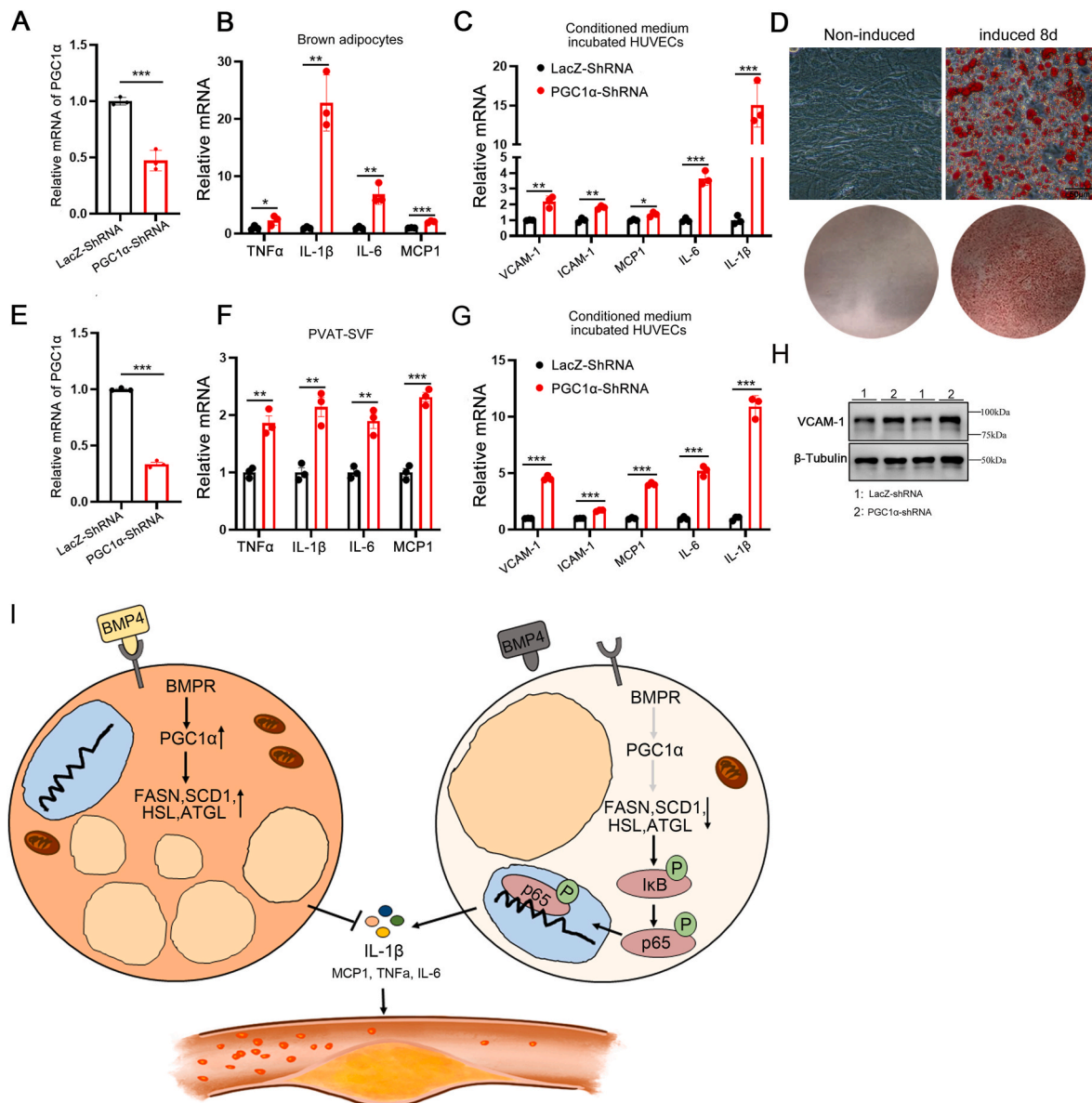


Fig. 8. BMP4 knockdown impairs PGC1 α mediated fatty acid metabolism and activates NF- κ B signaling in brown adipocytes. (A) Relative mRNA levels of PGC1 α in brown adipocytes with PGC1 α knockdown or lacZ knockdown. (B) Relative mRNA levels of TNF α , IL1 β , IL-6 and MCP1 in brown adipocytes with PGC1 α knockdown or lacZ knockdown. (C) Relative mRNA levels of VCAM-1, ICAM-1, MCP1, IL-6 and IL1 β were determined in TNF α pre-treated HUVEC incubated with conditioned medium from brown adipocyte with PGC1 α knockdown or lacZ knockdown. (D) Oil Red O staining of brown adipocytes differentiated from SVF on day 8. (E) Relative mRNA levels of PGC1 α in brown adipocytes differentiated from SVF with PGC1 α knockdown or lacZ knockdown. (F) Relative mRNA levels of TNF α , IL1 β , IL-6 and MCP1 brown adipocytes differentiated from SVF with PGC1 α knockdown or lacZ knockdown. (G) Relative mRNA levels of VCAM-1, ICAM-1, MCP1, IL-6 and IL1 β were determined in TNF α pre-treated HUVEC incubated with conditioned medium from brown adipocytes differentiated from SVF with PGC1 α knockdown or lacZ knockdown. (H) Western blot analysis of VCAM-1 expression in HUVECs incubated with conditioned medium from brown adipocytes differentiated from SVF with PGC1 α knockdown or lacZ knockdown. (I) Model illustrating the mechanism of BMP4-mediated adipocyte metabolism activation inhibit inflammation and atherosclerosis. BMP4 signaling activate PGC1 α , which erect positive effect on adipocyte lipid metabolism by promote genes expression of lipogenesis (FASN and SCD1) and lipolysis (HSL and ATGL). The active lipid metabolism inhibits adipocyte inflammation thereby reduces proinflammatory factors secretion. BMP4 deficiency disrupts this positive effect. Impaired lipid metabolism activates NF- κ B pathway thereby increases proinflammatory factors secretion which initiates HUVEC inflammation and leads to atherosclerosis. Values are means \pm S.E.M. *P < 0.05, **P < 0.01, ***P < 0.001 by unpaired Student's *t*-test (A to C, E to G). (For interpretation of the references to colour in this figure legend, the reader is referred to the Web version of this article.)

increase in proinflammatory gene expression (Fig. 8C). To further explore whether perivascular adipocytes play a key role in regulating HUVEC inflammation, we isolated stromal vascular fraction (SVF) cells from the PVAT of ApoE^{-/-} mice and induced them to differentiate into brown adipocytes (Fig. 8D). We knocked down PGC1 α expression in SVF with a PGC1 α shRNA (Fig. 8E) and observed induced expression of proinflammatory genes (Fig. 8F) and reduced expression of lipid metabolism-related genes (Fig. S7B). In addition, we incubated HUVECs with conditioned medium obtained from SVF with PGC1 α knockdown, which resulted in a significant increase in proinflammatory gene expression (Fig. 8G and H). These data indicate that PGC1 α knockdown in perivascular adipocytes recapitulates the *BMP4* knockdown phenotype of decreased fatty acid metabolism and increased adipocyte inflammation.

4. Discussion

Bone morphogenetic proteins (BMPs) were initially described as inducers of bone formation but are now also known to be involved in the development of adipose tissue and adipogenic differentiation [17,28]. BMP7 is most strongly linked to brown adipogenesis, as gene deletion of BMP7 in mice was shown to result in a 70% reduction in BAT at birth [29]. Mice with BAT specific deletion of BMPRIA, a receptor of BMP7 and BMP4 signaling, also demonstrated impaired cervical BAT formation [30]. However, overexpression of BMP4 in adipocytes was shown to activate the browning of white adipose tissue while inhibit the acquisition of a brown phenotype in brown adipose tissue [20,21]. Although the roles of BMP4 in WAT and BAT have been well studied, the role of BMP4 in PVAT is unknown. Here, we found that BMP4 is mostly expressed in PVAT and to a much lesser extent in BAT, demonstrating the important function of BMP4 in regulating the metabolism of PVAT. In humans, beige adipose tissue was found mainly in the neck, pericardial, surrounding the great vessels and around the kidney, while BAT found in the interscapular region has a predominant role in the infant [31]. Through clinical sample analysis, we documented that the expression of BMP4 is associated with browning in subcutaneous and pericardial adipose tissue, which were found to be an active beige fat through PET/CT [32].

Berbée et al. activated BAT using the β 3-AR agonist CL316243 in hyperlipidemic APOE*3-Leiden.CETP (E3L.CETP) mice, which have an intact apoE-LDLR pathway, and found that BAT activation accelerated plasma clearance and uptake of cholesterol-rich remnants by the liver [27]. Thus, activation of adipose tissue metabolism may be a potential target to combat atherosclerosis. Our previous study has shown that brown-related proteins were lower in CAD pericardial fat [15]. Here, we show that the expression of BMP4 in PVAT in atherosclerotic mice and patients with CAD decreased dramatically, suggesting that BMP4 in PVAT is closely associated with CAD. By contrasts, Dong et al. reported that cold induced BAT activation and browning of WAT enhanced lipolysis, which led to aggravated hypercholesterolemia and atherosclerosis development in ApoE^{-/-} and LDLR^{-/-} mice [33], suggesting that an intact apoE-LDLR pathway is necessary for the uptake of the formed triglyceride-rich lipoprotein (TRL) remnants. Therefore, a gentler way to promote browning of adipose tissue is needed to combat atherosclerosis. Our previous study found that BMP4 overexpression in adipose tissue stimulates adipocytes within beige cells in subcutaneous depots [20]. Using genetic engineering approaches to specifically ablate BMP4 in white or brown adipocytes, the expression of brown-related genes in PVAT was decreased, which resulted in the development of atherosclerosis. In addition, overexpression of BMP4 mediated activation of the PVAT metabolism, and, as such, the development of atherosclerosis was attenuated. These data indicate that the expression of BMP4 and brown-related genes in PVAT may have a regulatory effect on the development of atherosclerosis.

In BMP4 ^{Δ AP2} ApoE^{-/-} mice, we observed significantly increased levels of total cholesterol (TC) and low-density lipoprotein-cholesterol

(LDL-C) compared with the control mice; this is different from the results of our previous model, which demonstrated that mice with BMP4 deletion in adipocytes exhibited increased serum triglyceride levels but unchanged free fatty acid and cholesterol levels [20]. One possible reason for these differences is the ApoE^{-/-} genetic background. As elevated cholesterol is a contributing factor for atherosclerosis, the vascular phenotype of BMP4 ^{Δ AP2} ApoE^{-/-} mice at least partially resulted from systematic high level of cholesterol. However, although BMP4 ^{Δ UCP1} ApoE^{-/-} mice did not show an increase in TC and LDL-C levels, they still showed a significant increase in vascular inflammation and atherosclerosis development. Comparing BMP4 ^{Δ AP2} ApoE^{-/-} and BMP4 ^{Δ UCP1} ApoE^{-/-} mice, both models showed an approximately 2-fold increase in atherosclerotic plaques, which illustrated that the increase in TC and LDL-C in BMP4 ^{Δ AP2} ApoE^{-/-} did not contribute to more serious plaques. Moreover, overexpression of BMP4 activated PVAT metabolism and alleviated atherosclerosis without changing the level of plasma TC, TG, LDL and HDL. These data suggest that development of atherosclerosis in BMP4 ^{Δ AP2} ApoE^{-/-} mice is the result of high cholesterol level and local inflammation, while the development of atherosclerosis in BMP4 ^{Δ UCP1} ApoE^{-/-} mice only results from local inflammation. Taken together, our results highlight the importance of the direct local effect of PVAT on atherosclerosis.

According to the current view, cold induced BAT activation is accompanied by enhanced lipolysis [34]. Global or adipocyte specific ATGL knockout mice exhibited a lipolytic defect in BAT, and as a result, the mice were unable to maintain body temperature upon acute cold, leading to severe BAT hypertrophy due to TG accumulation [35]. Therefore, lipolysis is essential for cold-induced non-shivering thermogenesis, because BAT-derived fatty acids play a critical role in UCP1 activation and act as a primary fuel substrate [34]. Besides the activation of lipolysis, de novo lipogenesis (DNL) positively correlates with thermogenesis in BAT, as well as insulin sensitivity in WAT [36,37]. Sanchez-Gurmaches et al. showed that DNL is almost maximally induced when mice are transferred from thermoneutral conditions to room temperature, a mild cold stimulus for mice [38]. Here, we observed that knockout of BMP4 enlarged the size of adipocytes in PVAT, and down-regulated fatty acid metabolism related genes such as FASN, ACC, ATGL and HSL, which could reflect impaired PVAT fatty acid metabolism, involving both lipolysis and lipogenesis. PGC1 α , as an important transcriptional coactivator for the expression of UCP1, turns on several key components of the adaptive thermogenic program in brown fat, including fuel intake, fatty-acid oxidation, mitochondrial biogenesis, and increased oxygen consumption [39]. Here, we found that knockdown of PGC1 α in PVAT inhibited the expression of fatty acid metabolism related genes (Fig. S7B). Furthermore, we demonstrated that PGC1 α is a key factor in BMP4-mediated PVAT metabolism activation, which is similar to its role in mediating the BMP4-induced white-to-brown adipocyte shift.

Obesity-induced adipocyte hypertrophy promotes the synthesis and secretion of cytokines such as TNF α , interleukins (ILs), and C-C motif chemokine ligands (CCLs), which stimulate inflammation [40]. Adipose tissue inflammation is an emerging factor contributing to cardiovascular disease [41,42]. With regard to adipose tissue inflammation, much attention has been focused on the function of immune cells, while the "immune-like" function of adipocyte should be noted, which expresses various innate immune receptors and proinflammatory cytokines [43, 44]. IHC staining of F4/80 demonstrated that *BMP4* knockout PVAT exhibits more F4/80 positive macrophages per area, while BMP4 TG PVAT has fewer macrophages. Recent studies have shown that paracrine factors from local adipose tissues, that is, PVAT and pericardial adipose tissues, may be more directly associated with the development of CAD [45,46]. Here we demonstrate that BMP4 knockdown in perivascular adipocyte activates NF- κ B signaling, leading to the release of downstream proinflammatory factors, especially IL-1 β , which triggers endothelial inflammation and atherosclerosis.

Dyslipidemia and inflammation are pathological conditions that

damage the endothelium, triggering vascular remodeling and the development of atherosclerosis. In our data, we found that BMP4-regulated PVAT metabolism participates in the development of atherosclerosis largely through the local inflammatory changes rather than circulatory lipid alteration. In addition, our findings provide novel insights into the mechanisms by which BMP4 inhibits the expression of proinflammatory factors in perivascular adipocytes and has a direct anti-inflammatory effect on endothelial cells, thereby preventing the development of atherosclerosis. Therefore, targeting BMP4 in PVAT may represent a promising anti-inflammatory therapeutic strategy for atherosclerosis.

Author contributions

Y.T., W.J.M., and Q.-Q.T. designed the experiments and supervised the study; H.L. and Y.J.S. conducted experiments on human patient samples. W.J.M., S.W.Q., Y.J.S., L.J.Y., S.S.S., and D.N.P. carried out the animal and molecular experiments. W.J.M., S.W.Q., Y.T., Q.Q.Y., and Y.L. analyzed data; W.J.M. and Y.T. wrote the original draft. S.W.Q. and Q.-Q.T. reviewed and edited the paper.

Declaration of competing interest

All authors declare that there are no conflicts of interest.

Acknowledgements

We thank Z.H. Zao from Department of Pathology of School of Basic Medical Sciences, Fudan University for assistance with Frozen Sectioning technique. We appreciate H. Yin from Shanghai Institute of Nutrition and Health, University of Chinese Academy of Sciences, Chinese Academy of Sciences for providing mice expressing Cre recombinase under the control of brown adipocyte-specific promoter UCP1.

This study was supported by the National Natural Science Foundation of China (grant no. 81970754, 31701254 to Y.T., and grant no. 31670787 to S.-W.Q.), the ministry of science and technology of china grant (2018YFA0800401 to Q.-Q.T.) and the state key program of national natural science foundation of china (grant no. 81390353 to Q.-Q.T.). The research was partially supported by fund of peak disciplines (type IV) of institutions of higher learning in shanghai.

Appendix A. Supplementary data

Supplementary data to this article can be found online at <https://doi.org/10.1016/j.redox.2021.101979>.

References

- [1] K.J. Williams, I. Tabas, Atherosclerosis—an inflammatory disease, *N. Engl. J. Med.* 340 (1999) 1928, author reply 1929.
- [2] D. Wolf, K. Ley, Immunity and inflammation in atherosclerosis, *Circ. Res.* 124 (2019) 315–327.
- [3] P.K. Shah, Inflammation, infection and atherosclerosis, *Trends Cardiovasc. Med.* 29 (2019) 468–472.
- [4] Y. Zhu, X. Xian, Z. Wang, Y. Bi, Q. Chen, X. Han, D. Tang, R. Chen, Research progress on the relationship between atherosclerosis and inflammation, *Biomolecules* 8 (2018) 80.
- [5] P. Libby, The forgotten majority: unfinished business in cardiovascular risk reduction, *J. Am. Coll. Cardiol.* 46 (2005) 1225–1228.
- [6] C.S. Robbins, A. Chudnovskiy, P.J. Rauch, J. Figueiredo, Y. Iwamoto, R. Gorbatov, M. Etzrodt, G.F. Weber, T. Ueno, N. van Rooijen, M.J. Mulligan-Kehoe, P. Libby, M. Nahrendorf, M.J. Pittet, R. Weissleder, F.K. Swirski, Extramedullary hematopoiesis generates ly-6chigh monocytes that infiltrate atherosclerotic lesions, *Circulation* 125 (2012) 364–374.
- [7] F. Tacke, D. Alvarez, T.J. Kaplan, C. Jakubzick, R. Spanbroek, J. Llodra, A. Garin, J. Liu, M. Mack, N. van Rooijen, S.A. Lira, A.J. Habenicht, G.J. Randolph, Monocyte subsets differentially employ CCR2, CCR5, and CX3CR1 to accumulate within atherosclerotic plaques, *J. Clin. Invest.* 117 (2007) 185–194.
- [8] J.J. Fuster, N. Ouchi, N. Gokce, K. Walsh, Obesity-induced changes in adipose tissue microenvironment and their impact on cardiovascular disease, *Circ. Res.* 118 (2016) 1786–1807.
- [9] T.P. Fitzgibbons, S. Kogan, M. Aouadi, G.M. Hendricks, J. Straubhaar, M.P. Czech, Similarity of mouse perivascular and brown adipose tissues and their resistance to diet-induced inflammation, *Am. J. Physiol. Heart Circ. Physiol.* 301 (2011) H1425–H1437.
- [10] L. Chang, L. Villacorta, R. Li, M. Hamblin, W. Xu, C. Dou, J. Zhang, J. Wu, R. Zeng, Y.E. Chen, Loss of perivascular adipose tissue on peroxisome proliferator-activated receptor-gamma deletion in smooth muscle cells impairs intravascular thermoregulation and enhances atherosclerosis, *Circulation* 126 (2012) 1067–1078.
- [11] Z. Lin, X. Pan, F. Wu, D. Ye, Y. Zhang, Y. Wang, L. Jin, Q. Lian, Y. Huang, H. Ding, C. Triggie, K. Wang, X. Li, A. Xu, Fibroblast growth factor 21 prevents atherosclerosis by suppression of hepatic sterol regulatory element-binding protein-2 and induction of adiponectin in mice, *Circulation* 131 (2015) 1861–1871.
- [12] A. Bartelt, C. Weigelt, M.L. Cherradi, A. Niemeier, K. Tödter, J. Heeren, L. Scheja, Effects of adipocyte lipoprotein lipase on de novo lipogenesis and white adipose tissue browning, *Biochim. Biophys. Acta Mol. Cell Biol. Lipids* 1831 (2013) 934–942.
- [13] A. Bartelt, O.T. Bruns, R. Reimer, H. Hohenberg, H. Ittrich, K. Peldschus, M. G. Kaul, U.I. Tromsdorf, H. Weller, C. Waurisch, A. Eychemüller, P.L.S.M. Gordts, F. Rinninger, K. Bruegelmann, B. Freund, P. Nielsen, M. Merkel, J. Heeren, Brown adipose tissue activity controls triglyceride clearance, *Nat. Med.* 17 (2011) 200–205.
- [14] W. Xiong, X. Zhao, M.T. Garcia-Barrio, J. Zhang, J. Lin, Y.E. Chen, Z. Jiang, L. Chang, MitoNEET in perivascular adipose tissue blunts atherosclerosis under mild cold condition in mice, *Front. Physiol.* 8 (2017) 1032.
- [15] Y. Tang, Y. He, C. Li, W. Mu, Y. Zou, C. Liu, S. Qian, F. Zhang, J. Pan, Y. Wang, H. Huang, D. Pan, P. Yang, J. Mei, R. Zeng, Q. Tang, RPS3A positively regulates the mitochondrial function of human periaortic adipose tissue and is associated with coronary artery diseases, *Cell Discovery* 4 (2018), 52-17.
- [16] S. Kim, E. Lee, S. Lee, Y. Kim, C. Lee, D. Jo, S. Kim, Site-specific impairment of perivascular adipose tissue on advanced atherosclerotic plaques using multimodal nonlinear optical imaging, *Proceedings of the National Academy of Sciences - PNAS* 116 (2019) 17765–17774.
- [17] Q. Tang, T.C. Otto, M.D. Lane, Commitment of C3H10T1/2 pluripotent stem cells to the adipocyte lineage, *Proceedings of the National Academy of Sciences - PNAS* 101 (2004) 9607–9611.
- [18] R. Xue, Y. Wan, S. Zhang, Q. Zhang, H. Ye, Y. Li, Role of bone morphogenetic protein 4 in the differentiation of brown fat-like adipocytes, *Am. J. Physiol. Endocrinol. Metabol.* 306 (2014) E363–E372.
- [19] M. Elsen, S. Raschke, N. Tennagels, U. Schwahn, T. Jelenik, M. Roden, T. Romacho, J. Eckel, BMP4 and BMP7 induce the white-to-brown transition of primary human adipose stem cells, *Am. J. Physiol. Cell Physiol.* 306 (2014) C431–C440.
- [20] S. Qian, Y. Tang, X. Li, Y. Liu, Y. Zhang, H. Huang, R. Xue, H. Yu, L. Guo, H. Gao, Y. Liu, X. Sun, Y. Li, W. Jia, Q. Tang, BMP4-mediated brown fat-like changes in white adipose tissue alter glucose and energy homeostasis, *Proc. Natl. Acad. Sci. Unit. States Am.* 110 (2013) E798–E807.
- [21] S. Modica, L.G. Straub, M. Balaz, W. Sun, L. Varga, P. Stefanicka, M. Profant, E. Simon, H. Neubauer, B. Ukropcova, J. Ukropec, C. Wolfrum, Bmp4 promotes a Brown to white-like adipocyte shift, *Cell Rep.* 16 (2016) 2243–2258.
- [22] J.M. Hoffmann, J.R. Grünberg, C. Church, I. Elias, V. Palsdottir, J. Jansson, F. Bosch, A. Hammarstedt, S. Hedjazifar, U. Smith, O.N.A.P. Institute, D.O.M. A. Institute of Medicine, U. Göteborgs, U. Gothenburg, A. Sahlgrenska, A. Sahlgrenska, A.F.M.O. Institutionen För Medicin, F.N.O.F. Institutionen, BMP4 gene therapy in mature mice reduces BAT activation but protects from obesity by browning subcutaneous adipose tissue, *Cell Rep.* 20 (2017) 1038–1049.
- [23] D. Pan, L. Huang, L.J. Zhu, T. Zou, J. Ou, W. Zhou, Y. Wang, Mjrd3-Mediated H3K27me3 dynamics orchestrate Brown fat development and regulate white fat plasticity, *Dev. Cell* 35 (2015) 568–583.
- [24] X.Y. Tian, K. Ganesan, C. Hong, K.D. Nguyen, Y. Qiu, J. Kim, R.K. Tangirala, P. Tontonoz, A. Chawla, Thermoneutral housing accelerates metabolic inflammation to potentiate atherosclerosis but not insulin resistance, *Cell Metabol.* 23 (2016) 165–178.
- [25] P. Libby, J.E. Buring, L. Badimon, G.K. Hansson, J. Deanfield, M.S. Bittencourt, L. Tokgozoglu, E.F. Lewis, Atherosclerosis, *Nat Rev Dis Primers.* 5 (2019) 56.
- [26] W.D. Tucker, Y. Arora, K. Mahajan, Anatomy, Blood Vessels, 2020.
- [27] J.F. Berbee, M.R. Boon, P.P. Khedoe, A. Bartelt, C. Schlein, A. Worthmann, S. Kooijman, G. Hoeke, I.M. Mol, C. John, C. Jung, N. Vazirpanah, L.P. Brouwers, P. L. Gordts, J.D. Esko, P.S. Hiemstra, L.M. Havekes, L. Scheja, J. Heeren, P.C. Rensen, Brown fat activation reduces hypercholesterolaemia and protects from atherosclerosis development, *Nat. Commun.* 6 (2015) 6356.
- [28] T.J. Schulz, Y. Tseng, Emerging role of bone morphogenetic proteins in adipogenesis and energy metabolism, *Cytokine Growth Factor Rev.* 20 (2009) 523–531.
- [29] Y.H. Tseng, E. Kokkotou, T.J. Schulz, T.L. Huang, J.N. Winnay, C.M. Taniguchi, T. Tran, R. Suzuki, D.O. Espinoza, Y. Yamamoto, M.J. Ahrens, A.T. Dudley, A. W. Norris, R.N. Kulkarni, C.R. Kahn, New role of bone morphogenetic protein 7 in brown adipogenesis and energy expenditure, *Nature* 454 (2008) 1000–1004.
- [30] T.J. Schulz, P. Huang, T.L. Huang, R. Xue, L.E. McDougall, K.L. Townsend, A. M. Cypess, Y. Mishina, E. Gussoni, Y.H. Tseng, Brown-fat paucity due to impaired BMP signalling induces compensatory browning of white fat, *Nature* 495 (2013) 379–383.
- [31] L.W. van Marken, J.W. Vanhommerig, N.M. Smulders, J.M. Drossaerts, G. J. Kemerink, N.D. Bouvy, P. Schrauwen, G.J. Teule, Cold-activated brown adipose tissue in healthy men, *N. Engl. J. Med.* 360 (2009) 1500–1508.

- [32] L.Y.I. Yamaga, L.Y.I. Yamaga, A.F. Thom, A.F. Thom, J. Wagner, J. Wagner, R. H. Baroni, R.H. Baroni, J.T. Hidal, J.T. Hidal, M.G. Funari, M.G. Funari, The effect of catecholamines on the glucose uptake in brown adipose tissue demonstrated by 18F-FDG PET/CT in a patient with adrenal pheochromocytoma, *Eur. J. Nucl. Med. Mol. Imag.* 35 (2008) 446–447.
- [33] M. Dong, X. Yang, S. Lim, Z. Cao, J. Honek, H. Lu, C. Zhang, T. Seki, K. Hosaka, E. Wahlberg, J. Yang, L. Zhang, T. Länne, B. Sun, X. Li, Y. Liu, Y. Zhang, Y. Cao, Cold exposure promotes atherosclerotic plaque growth and instability via UCP1-dependent lipolysis, *Cell Metabol.* 18 (2013) 118–129.
- [34] B. Cannon, J. Nedergaard, Brown adipose tissue: function and physiological significance, *Physiol. Rev.* 84 (2004) 277–359.
- [35] G. Haemmerle, Defective lipolysis and altered energy metabolism in mice lacking adipose triglyceride lipase, *Science (American Association for the Advancement of Science)* 312 (2006) 734–737.
- [36] A. Takahashi, T. Shimazu, Stimulation of hypothalamic nuclei has differential effects on lipid synthesis in brown and white adipose tissue, *Nature (London)* 284 (1980) 62–63.
- [37] Y. Tang, M. Wallace, J. Sanchez-Gurmaches, W. Hsiao, H. Li, P.L. Lee, S. Vernia, C. M. Metallo, D.A. Guertin, Adipose tissue mTORC2 regulates ChREBP-driven de novo lipogenesis and hepatic glucose metabolism, *Nat. Commun.* 7 (2016), 11365–11365.
- [38] J. Sanchez-Gurmaches, Y. Tang, N.Z. Jespersen, M. Wallace, C. Martinez Calejman, S. Gujja, H. Li, Y.J.K. Edwards, C. Wolfrum, C.M. Metallo, S. Nielsen, C. Scheele, D. A. Guertin, Brown fat AKT2 is a cold-induced kinase that stimulates ChREBP-mediated de novo lipogenesis to optimize fuel storage and thermogenesis, *Cell Metabol.* 27 (2018) 195–209.e6.
- [39] Z. Wu, P. Puigserver, U. Andersson, C. Zhang, G. Adelmant, V. Mootha, A. Troy, S. Cinti, B. Lowell, R.C. Scarpulla, B.M. Spiegelman, Mechanisms controlling mitochondrial biogenesis and respiration through the thermogenic coactivator PGC-1, *Cell* 98 (1999) 115–124.
- [40] L.C. Freitas Lima, V.D.A. Braga, M. Do Socorro De França Silva, J.D.C. Cruz, S. H. Sousa Santos, M.M. de Oliveira Monteiro, C.D.M. Balarini, Adipokines, diabetes and atherosclerosis: an inflammatory association, *Front. Physiol.* 6 (2015).
- [41] A.D. Dobrian, M.A. Hatcher, J.J. Brotman, E.V. Galkina, P. Taghavi-Moghadam, H. Pei, B.A. Haynes, J.L. Nadler, Signal transducer and activator of transcription 4 contributes to adipose tissue inflammation and atherosclerosis, *J. Endocrinol.* 227 (2015) 13–24.
- [42] C. Li, S. Li, F. Zhang, M. Wu, H. Liang, J. Song, C. Lee, H. Chen, Endothelial microparticles-mediated transfer of microRNA-19b promotes atherosclerosis via activating perivascular adipose tissue inflammation in apoE(-/-) mice, *Biochem. Biophys. Res. Commun.* 495 (2018) 1922–1929.
- [43] L.A.J. O'Neill, D. Golenbock, A.G. Bowie, The history of Toll-like receptors — redefining innate immunity, *Nat. Rev. Immunol.* 13 (2013) 453–460.
- [44] D. Frasca, A. Diaz, M. Romero, S. Thaller, B.B. Blomberg, Secretion of autoimmune antibodies in the human subcutaneous adipose tissue, *PloS One* 13 (2018), e0197472.
- [45] N.K. Brown, Z. Zhou, J. Zhang, R. Zeng, J. Wu, D.T. Eitzman, Y.E. Chen, L. Chang, Perivascular adipose tissue in vascular function and disease: a review of current research and animal models, *Arterioscler. Thromb. Vasc. Biol.* 34 (2014) 1621–1630.
- [46] X.Y. Qi, S.L. Qu, W.H. Xiong, O. Rom, L. Chang, Z.S. Jiang, Perivascular adipose tissue (PVAT) in atherosclerosis: a double-edged sword, *Cardiovasc. Diabetol.* 17 (2018) 134.